The 23rd International Conference on Few-Body Problems in Physics (FB23)

# $\pi^0\pi^0$ femtoscopy in photoproduction at $E_\gamma < 2.4$ GeV

Qinghua HE (NUAA)
H. Shimizu (Tohoku U.)
for BGOegg collaboration

@Beijing, September 22-27, 2024

# Outline

§ Why photoproduction?

§ BGOegg experiments

- Setup
- Selected physics topics

§ $\pi^0\pi^0$ correlations

- Motivation
- Event selection
- correlation function

§ Discussion

§ Summary

# Why photoproduction?

## Hadron spectroscopy

-Still many quark models predicted resonances are missing for excited baryons (W>2 GeV)

-Mass ordering problem (e.g. N(1440) and N(1535))

**GeV Photon probe is promising for searching these missing resonances**

**Meson photoproduction**

**$\gamma N \rightarrow N^{*} or \Delta^{*} \rightarrow$ mesons N for light baryon spectroscopy**

**-Short-lived resonances are overlapped with each other**

BGOegg ($E_\gamma$ =1.3-2.4 GeV)

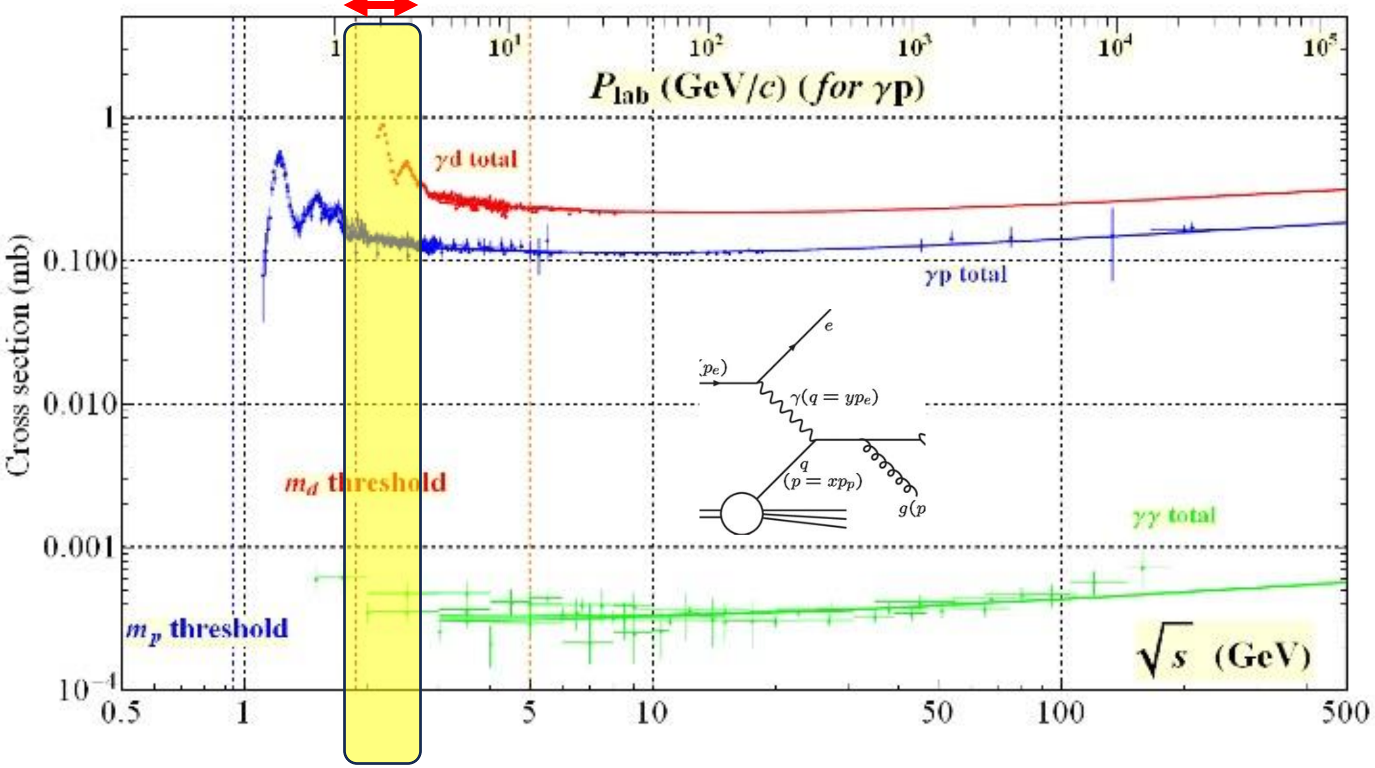

# BGOegg experiment | setup


A large acceptance electromagnetic (EM) calorimeter BGOegg (Fig.1) was constructed at ELPH, Tohoku University. This calorimeter system has been transferred to the new laser Compton scattering beamline LEPS2 at SPring-8, where a 1.3-2.9 GeV photon beam with high linear polarization is available. The phase-1 experiments have started from 2014 April with the EM calorimeter BGOegg and the additional detectors for charged particles. We are now upgrading the experimental setup by covering most of the solid angles with EM calorimeters to start new data collection in the phase-2 experiments.

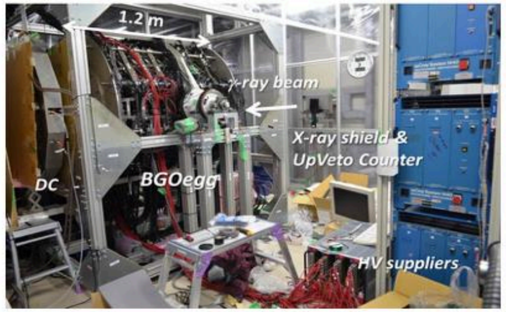


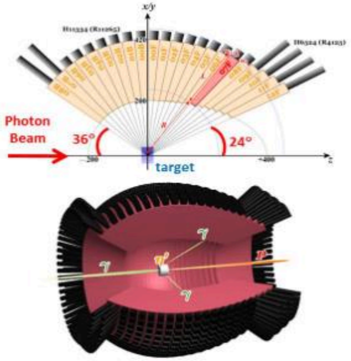


Fig.1 A picture of BGOegg inside the thermostatic booth (Left) and the drawings of BGOegg (Right).

## Physics

experiments, we are planning to upgrade the detector setup as shown in Fig.3. Instead of using DC and RPC, the forward acceptance hole of the BGOegg calorimeter will be covered by additional EM calorimeters. We install the "Forward Gamma" detector, which consists of 252 PWO crystals, in the polar angle range of 3 to 16 degrees. We are also considering to cover the gap region between the BGOegg calorimeter and the Forward Gamma detector. This configuration will significantly reduce backgrounds in the direct measurement of η'-mass spectral shape using a nuleus target.

## Status

The LEPS2/BGOegg experiments are carried out under the collaboration of ELPH (Tohoku University), RCNP (Osaka University), Nanjing University of Aeronautics and Astronautics, Kyoto University, KEK, RIKEN, JASRI (SPring-8), and many other institutes in the world. ELPH and RCNP cooperate the LEPS2 facility.

# BGOegg experiment | setup

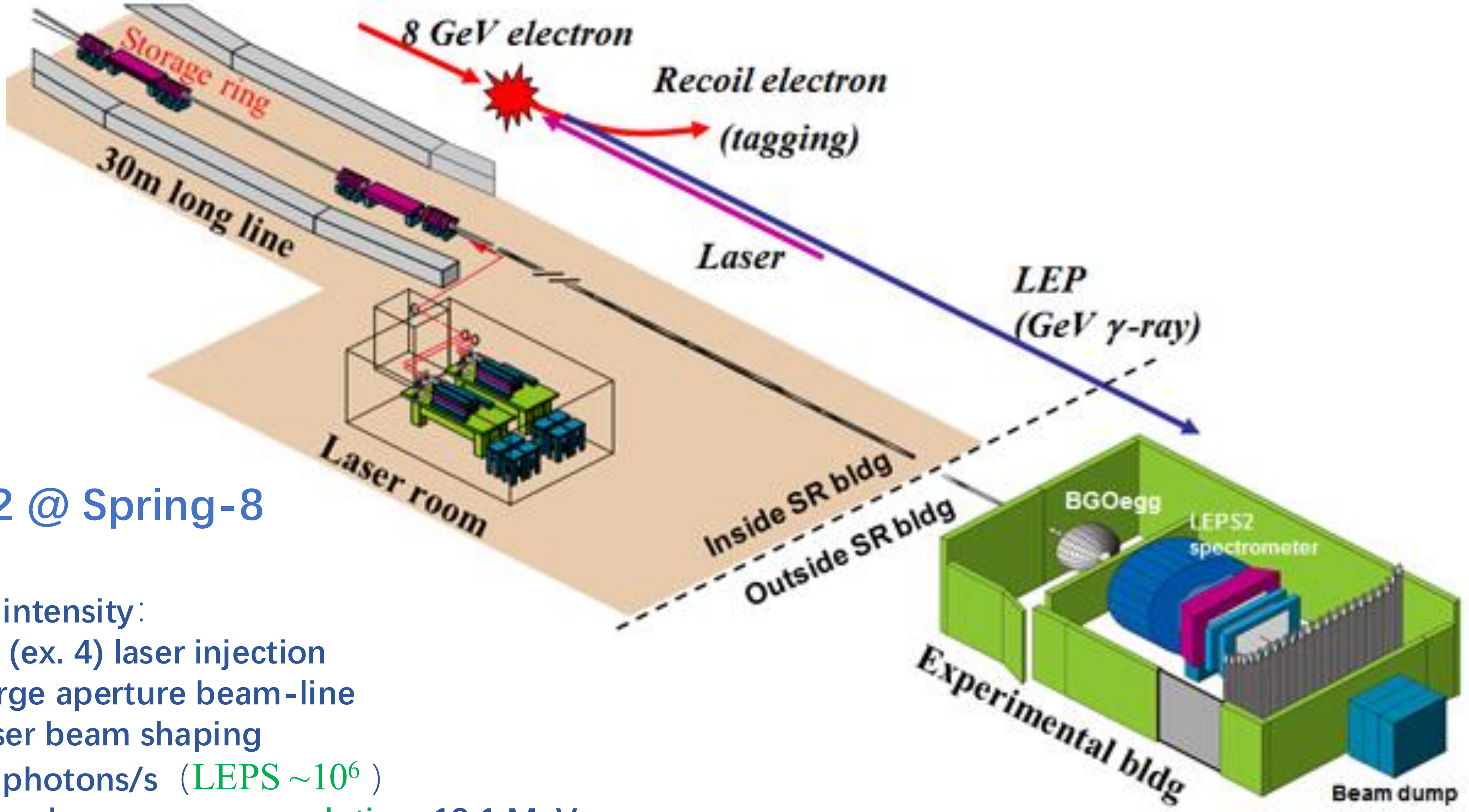


## LEPS2 @ Spring-8

High intensity:
Multi (ex. 4) laser injection
w/ large aperture beam-line
& Laser beam shaping
~$10^7$ photons/s (LEPS ~$10^6$ )
Photon-beam energy resolution: 12.1 MeV

# BGOegg experiment | setup

**World leading energy resolution ($\pi^0$ mass resolution: 6.7 MeV/$c^2$; $\eta$: 14.4 MeV/$c^2$)**

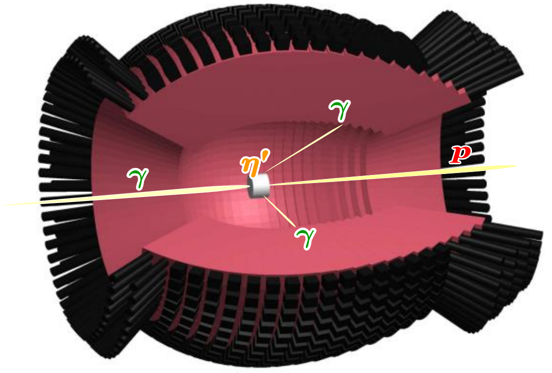


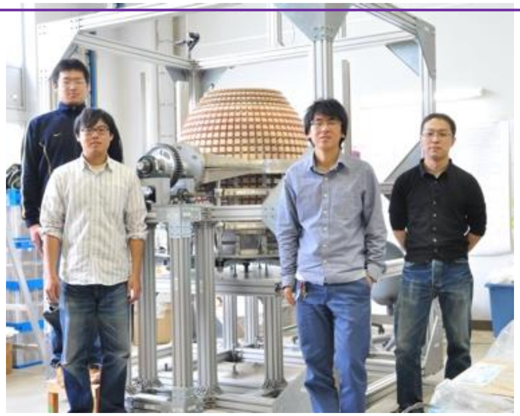

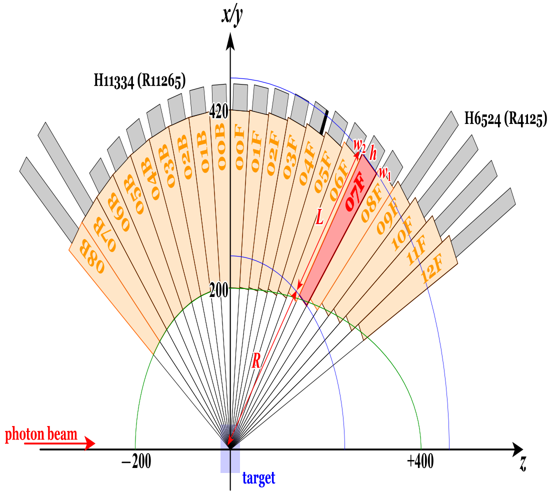


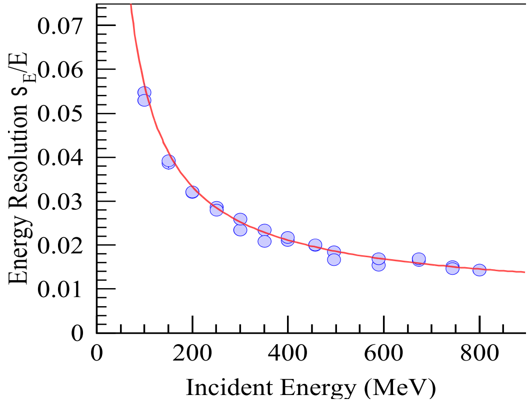


Target: LH2 (54mm) or Carbon (20 mm)

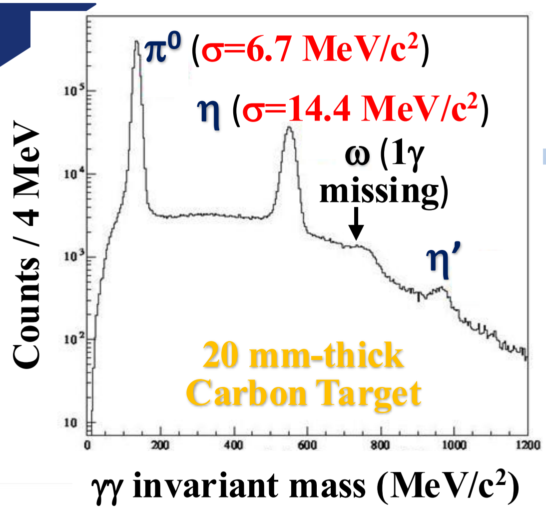


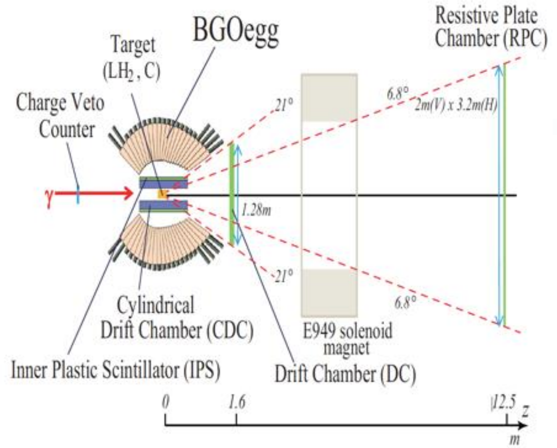


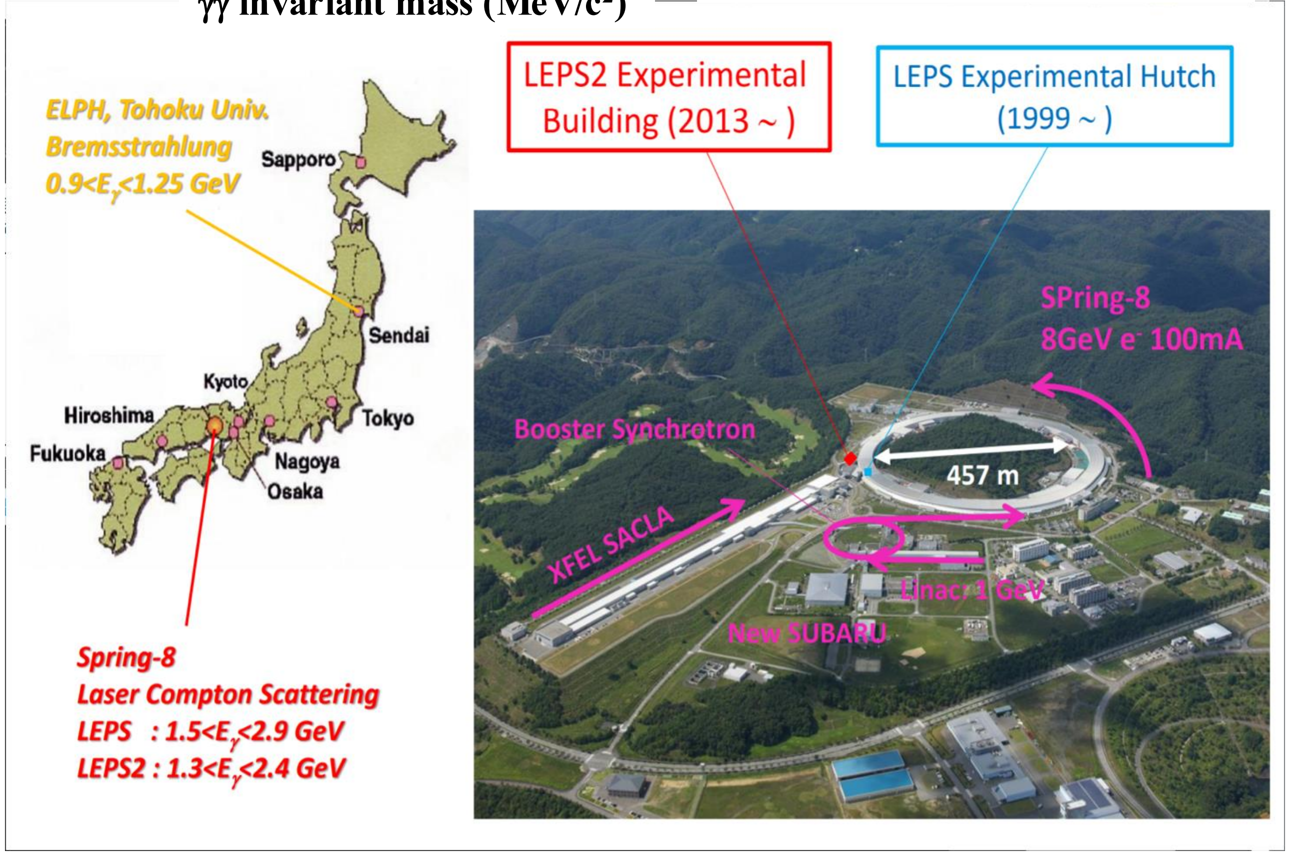


*M. Miyabe, N. Muramatsu, H. Shimizu, et al., NIM paper in preparation.*

# BGOegg experiment | setup

## FOREST EM Calorimeter

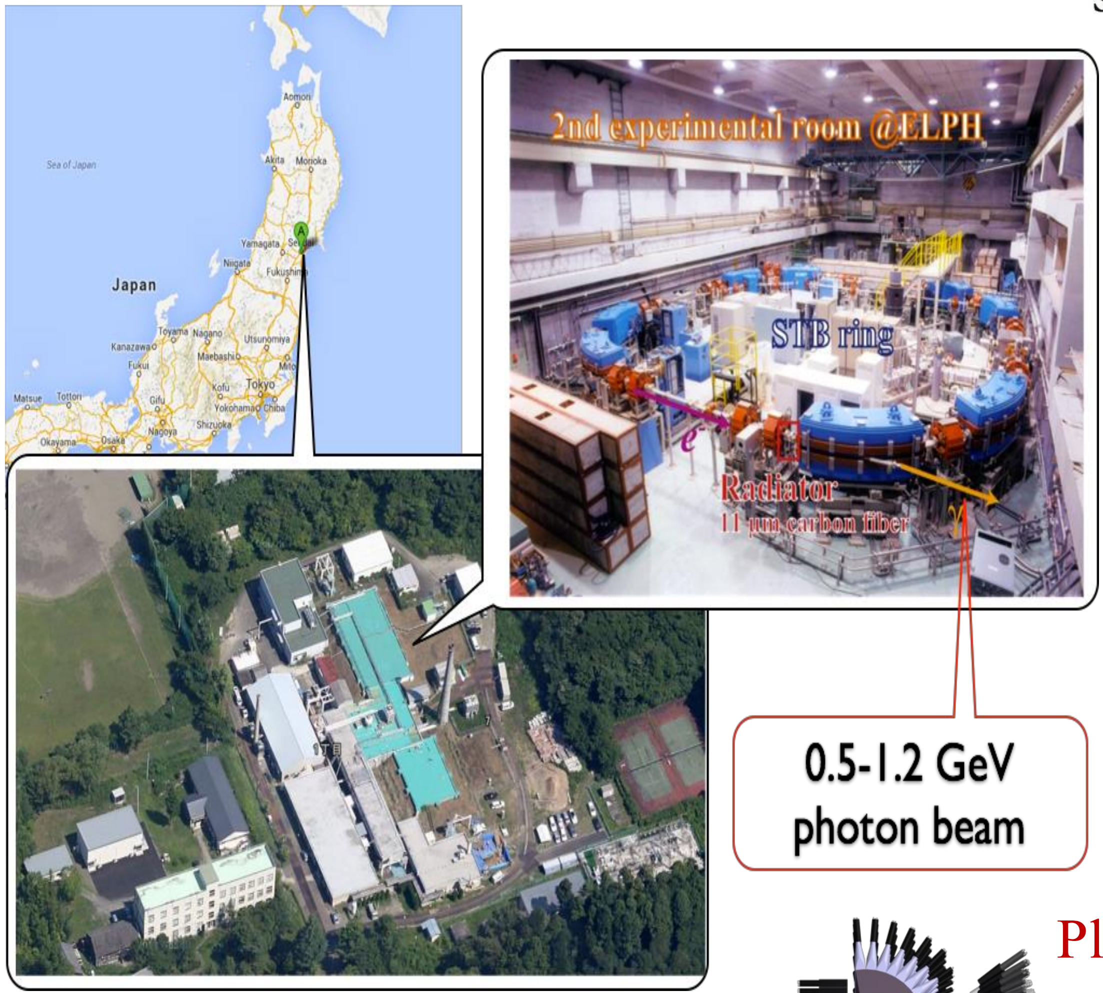


SCISSORS III

SPIDER

LEPS Backward Gamma

IVY

LOTUS

Rafflesia II

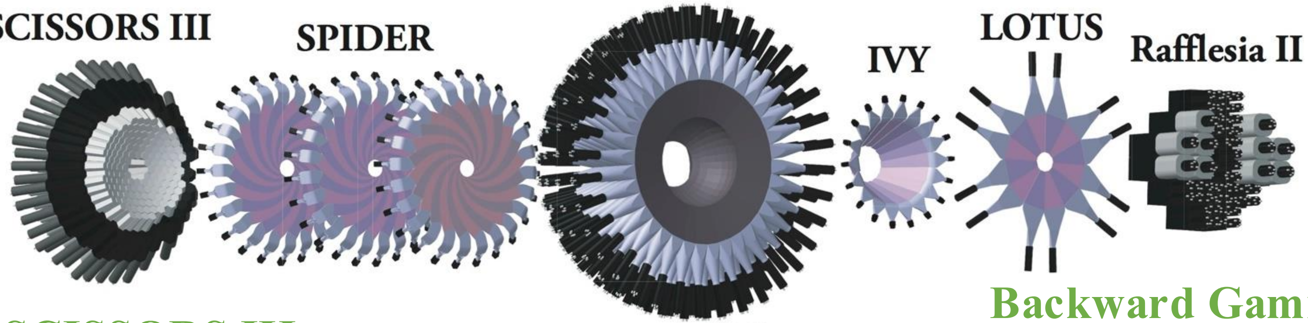

**SCISSORS III**

192 CsI; θ: 4°-24°, φ:full

Res. : 3% @ 1GeV

**Backward Gamma**

252 Lead/Scintillating fiber modules;

θ: 30°-100°, φ:full

Res. : 7% @ 1GeV

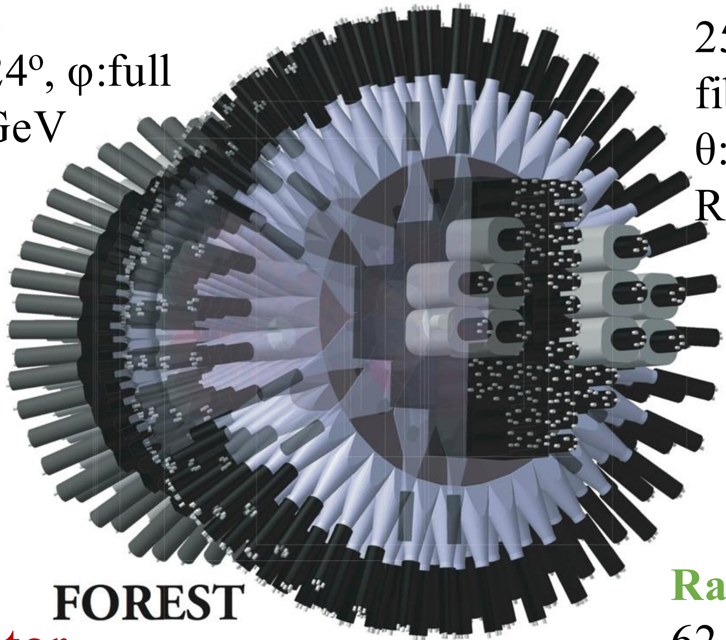

FOREST

**Rafflesia II**

62 Lead Glass modules;

Res. : 5% @ 1GeV

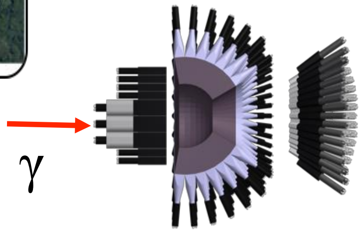


Plastic Scintillator

SPIDER (2 layers × 24 modules

IVY (18 modules)

LOTUS (12 modules)

# BGOegg experiment | Selected physics topics

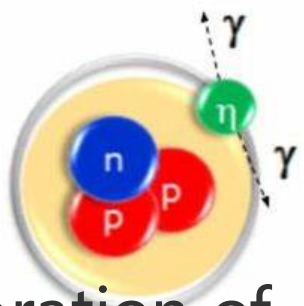

³He-η bound state

## ☐ Search for η' mesic nuclei

- mass reduction of 80-150 MeV at nuclear density (partial restoration of chiral symmetry inside high-density condition)
- bound η' mesic nuclei in the C(γ,p)X reaction.

N. Tomida, N. Muramatsu,M. Niiyama, et al. (BGOegg), Phys. Rev. Lett. **124**, 202501 (2020).

## ☐ Differential cross-section and beam asymmetry of the neutral mesons

The production of mesons from liquid hydrogen targets is suitable for investigating the excitation states of nucleons.

N. Muramatsu, S. K. Wang, Q. H. He , et al. (BGOegg), Phys. Rev. C 107, L042201 (2023)
Q. H. He, N. Muramatsu, SPring-8/SACLA Research Frontiers 2023 (2024)

## ☐ In-medium effect of the spectral shape of η'

- The width of η' may change
- Aaccurately measuring the spectrum of η'

# BGOegg experiment | Selected physics topics

## Hadron mass origin

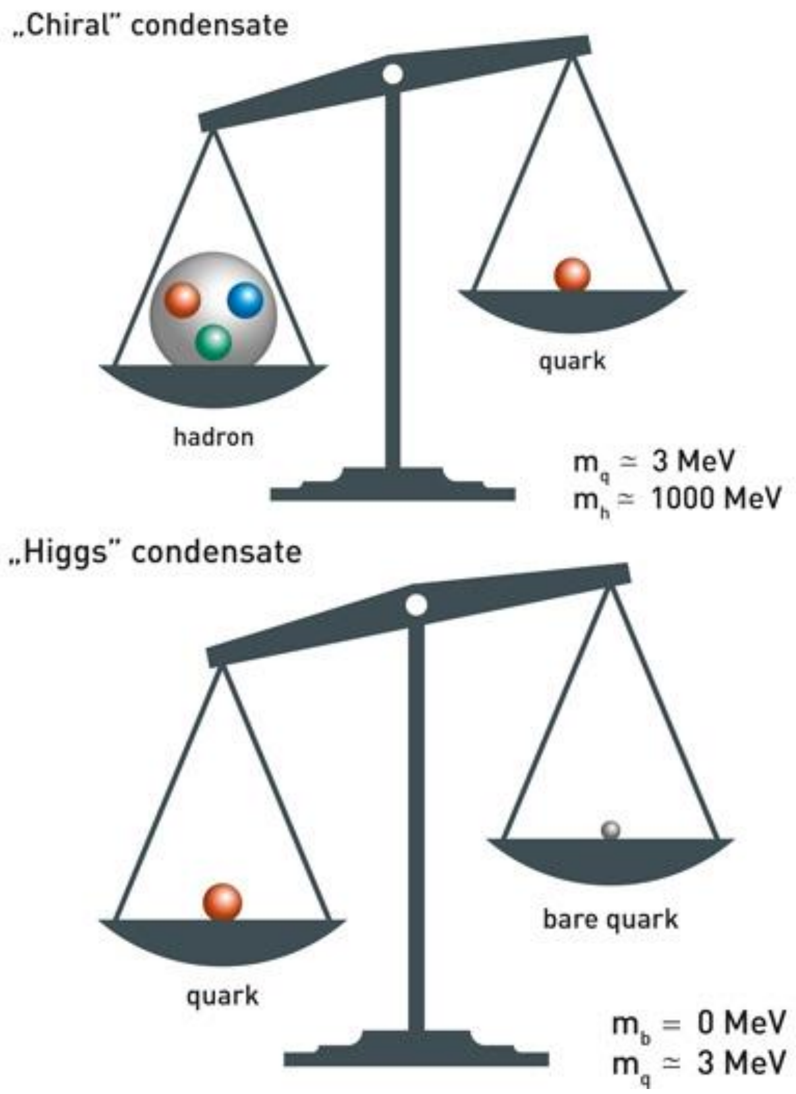


**Yukawa coupling and Higgs particles explain the fundamental fermions masses, while the hadron mass is generated by the strong interaction in QCD。**

Chiral symmetry breaking plays a key role to explain light hadrons masses

$U_A(1)$ symmetry breaking → $\eta'(985)$ exceptionally large mass
Mass gap between $\eta'$ and η

Search for **the in-medium mass reduction of η′** (partial restoration of spontaneous chiral symmetry breaking may weaken the anomaly effect)

Nambu-Jona-Lasinio and linear sigma models containing an $U_A(1)$ symmetry breaking term → predict → 150 and 80 MeV mass reduction

# BGOegg experiment | Selected physics topics

## Hadron mass origin

- The mass reduction is described as an attractive potential for an $\eta'$ meson in a nucleus
- ***$\eta'$*-nucleus bound states** can be formed.
- To search for $\eta'$ -nucleus bound states, we used missing-mass spectroscopy of the $^{12}C(\gamma,p)$ reaction detecting decay products in coincidence.

$$E_{\text{ex}} - E_0^{\eta'} = MM[^{12}\text{C}(\gamma, p_f)] - M_{^{11}\text{B}} - M_{\eta'}$$

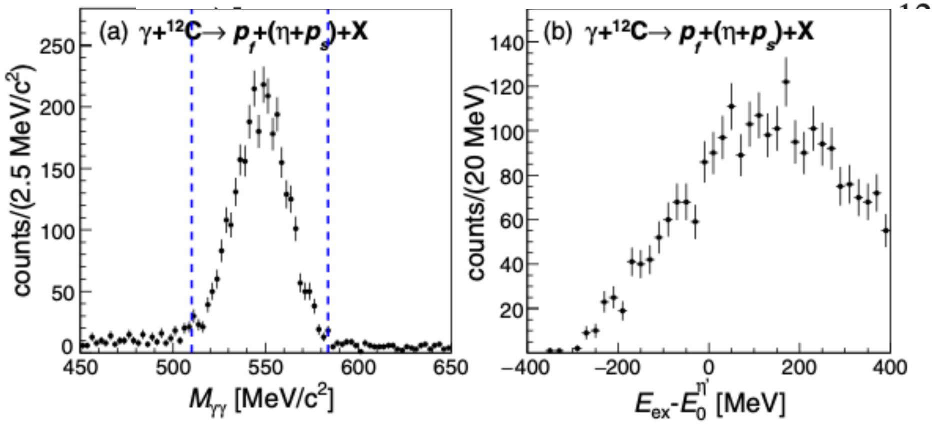


FIG. 1. (a) The $2\gamma$ invariant mass distribution around the $\eta$ mass and (b) the excitation function of the $(\eta + p_s)$ coincidence data. The region in $\pm 2.5\sigma$ from the invariant mass peak is indicated by the blue-dashed lines.

We measured missing mass spectrum of the $^{12}\text{C}(\gamma, p)$ reaction for the first time in coincidence with potential decay products from $\eta'$ bound nuclei. We tagged an $(\eta + p)$ pair associated with the $\eta' N \to \eta N$ process in a nucleus. After applying kinematical selections to reduce backgrounds, no signal events were observed in the bound-state region. An upper limit of the signal cross section in the opening angle $\cos\theta_{\text{lab}}^{\eta p} < -0.9$ was obtained to be 2.2 nb/sr at the 90% confidence level. It is compared with theoretical cross sections, whose normalization ambiguity is suppressed by measuring a quasifree $\eta'$ production rate. Our results indicate a small branching fraction of the $\eta' N \to \eta N$ process and/or a shallow $\eta'$-nucleus potential.

DOI: 10.1103/PhysRevLett.124.202501

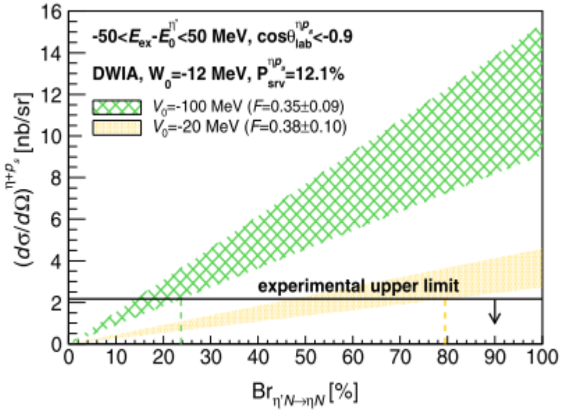


FIG. 4. The experimental upper limit of $(d\sigma/d\Omega)_{\text{exp}}^{\eta+p_s}$ at the 90% confidence level, and $(d\sigma/d\Omega)_{\text{theory}}^{\eta+p_s}$ as a function of $\text{Br}_{\eta' N\to\eta N}$.

N. Tomida, N. Muramatsu,M. Niiyama, et al. (BGOegg), Phys. Rev. Lett. **124**, 202501 (2020).

# BGOegg experiment | Selected physics topics

$\gamma p \rightarrow f_0(980)p \rightarrow \pi^0\pi^0 p$

$@E_\gamma = 1.3\sim2.4$ GeV

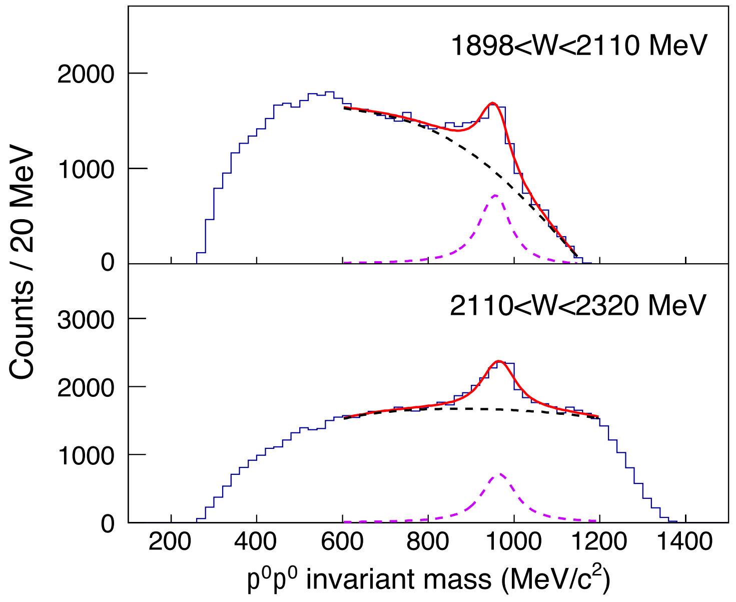


Invariant mass spectra of $\pi^0\pi^0$ in two energy bins. Voigt functions are fitted with polynomial background functions to extract $f_0(980)$ signals.

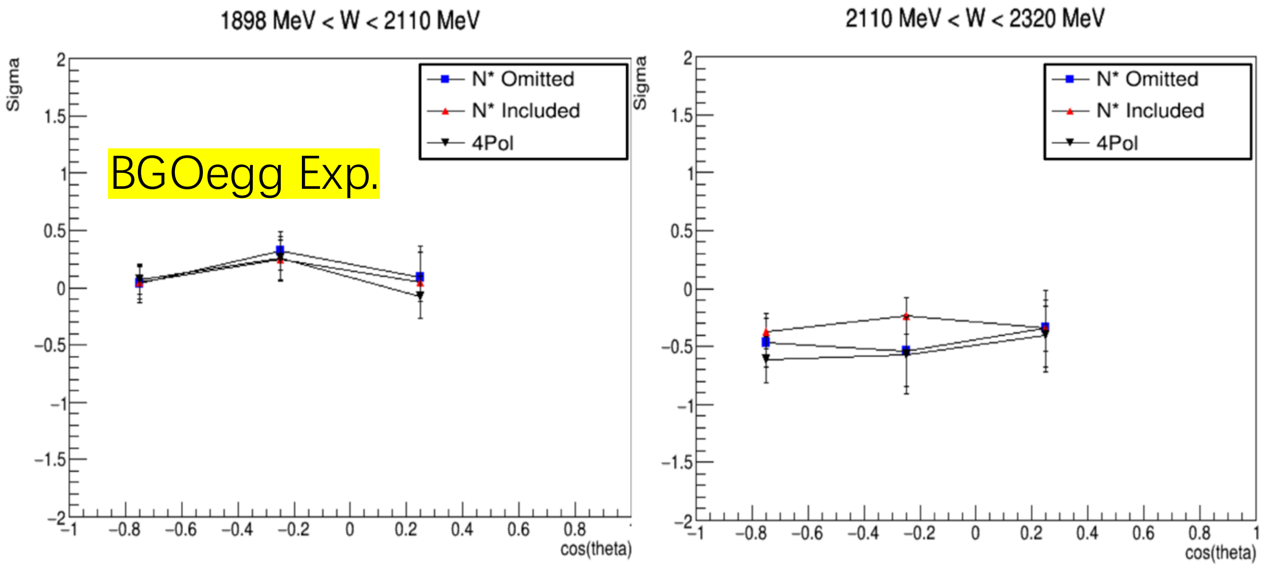


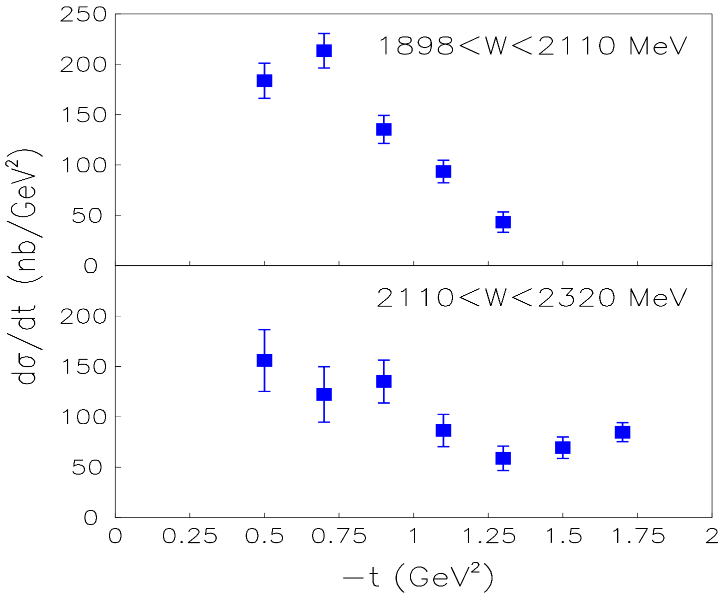


Differential cross sections $d\sigma/dt$

$$P_\gamma \Sigma / f_{int} = (N_{perp} - N_{para})/(N_{perp} + N_{para})$$

$$N_{perp} = \int_{\pi/4}^{3/4\pi} \frac{d\sigma_0}{d\Omega}(1 - P_\gamma \Sigma \cos 2\Phi)d\Phi + \int_{5/4\pi}^{7/4\pi} \frac{d\sigma_0}{d\Omega}(1 - P_\gamma \Sigma \cos 2\Phi)d\Phi$$

$$N_{para} = \int_{-\pi/4}^{\pi/4} \frac{d\sigma_0}{d\Omega}(1 - P_\gamma \Sigma \cos 2\Phi)d\Phi + \int_{3/4\pi}^{5/4\pi} \frac{d\sigma_0}{d\Omega}(1 - P_\gamma \Sigma \cos 2\Phi)d\Phi,$$

$f_{int} = \pi/2$ : correction factor for the integration over $\pi/2$ azimuthal angle ranges

- N. Muramatsu, S. K. Wang, Q. H. He , et al. (BGOegg), Phys. Rev. C 107, L042201 (2023)
- Q. H. He, N. Muramatsu, SPring-8/SACLA Research Frontiers 2023 (2024)

# $\pi^0\pi^0$ correlations | Motivation

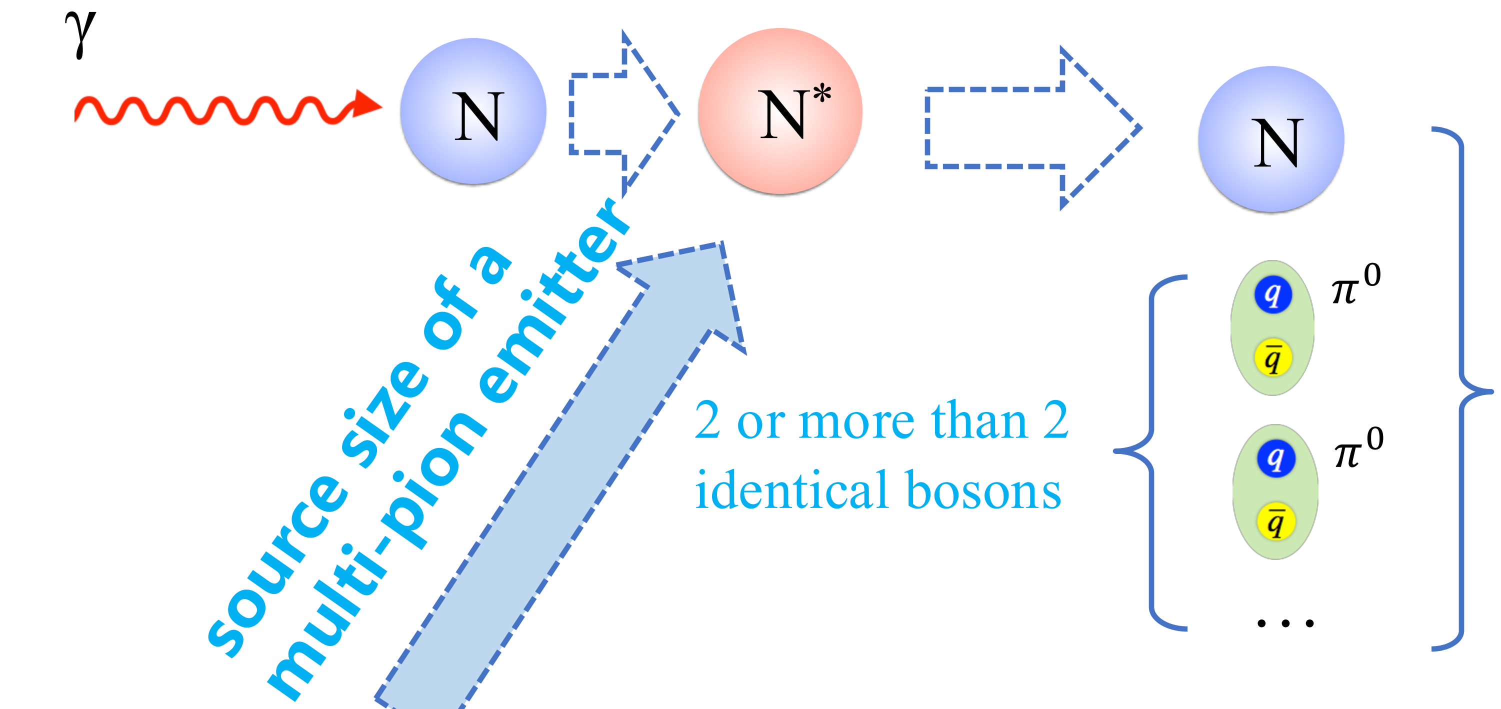



**$\gamma p \to \pi^0\pi^0 p$**

1.3-2.4 GeV

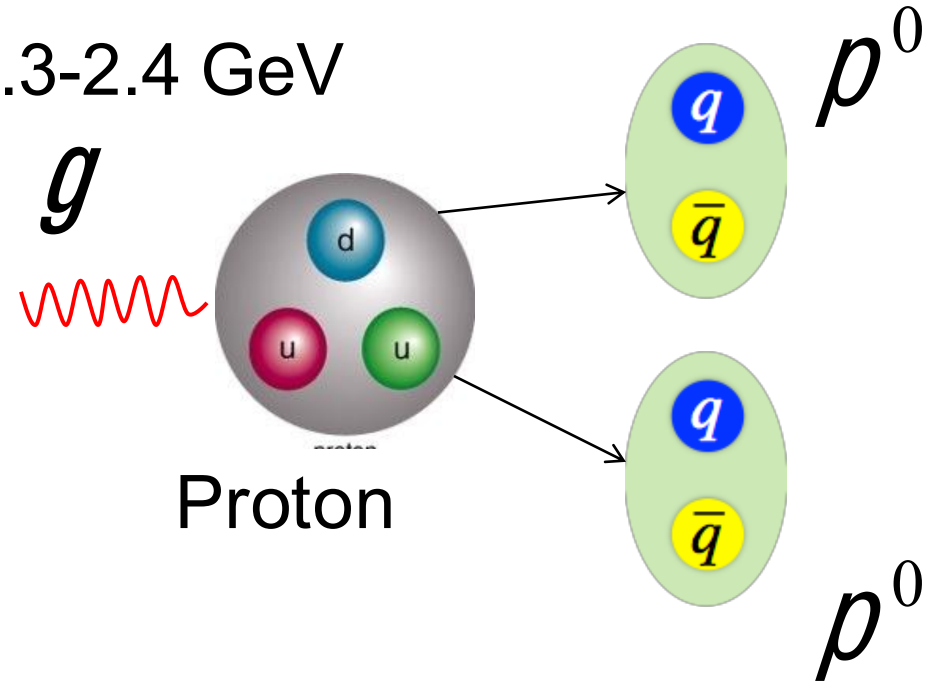


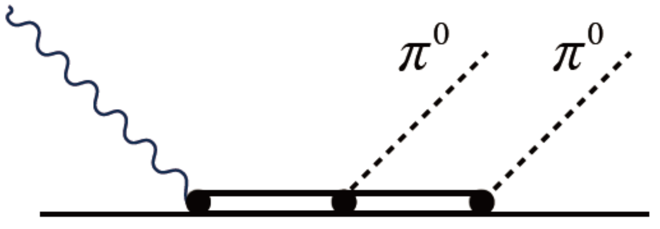


**<u>Intensity interference</u>** between identical particles (**HBT effects**) provides a tool to measure the space-time properties of the particle emission source.

# $\pi^0\pi^0$ correlations | Motivation

## Hanbury Brown-Twiss (HBT) effects

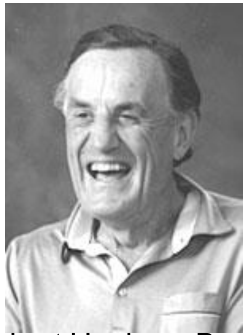


Robert Hanbury Brown 1916-2002

Richard Quentin Twiss 1920-2005

Australian Academy of Science

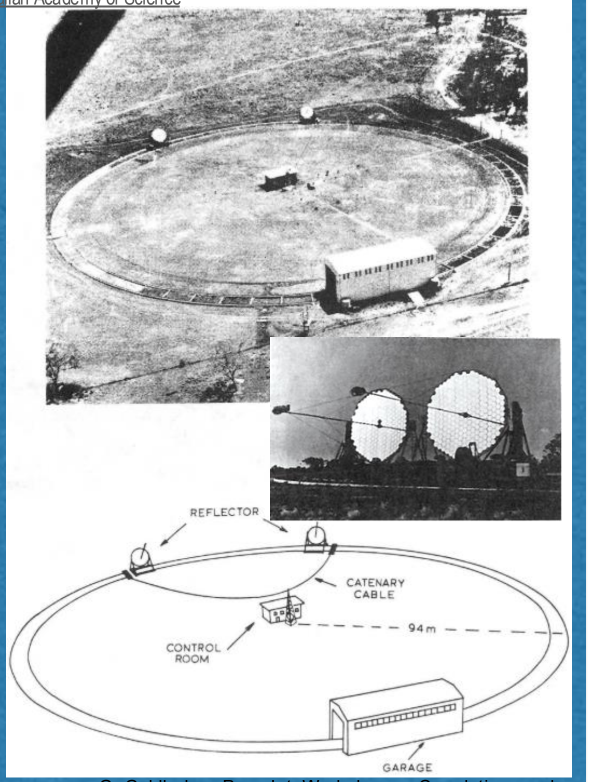


source: G. Goldhaber, Proc. Int. Workshop on Correlations and Mul- tiparticle production (CAMP - LESIP IV), p. 409, ed. by M L Plümer, S Raha and R M Weiner, World Scientific (1991).

2024/9/26

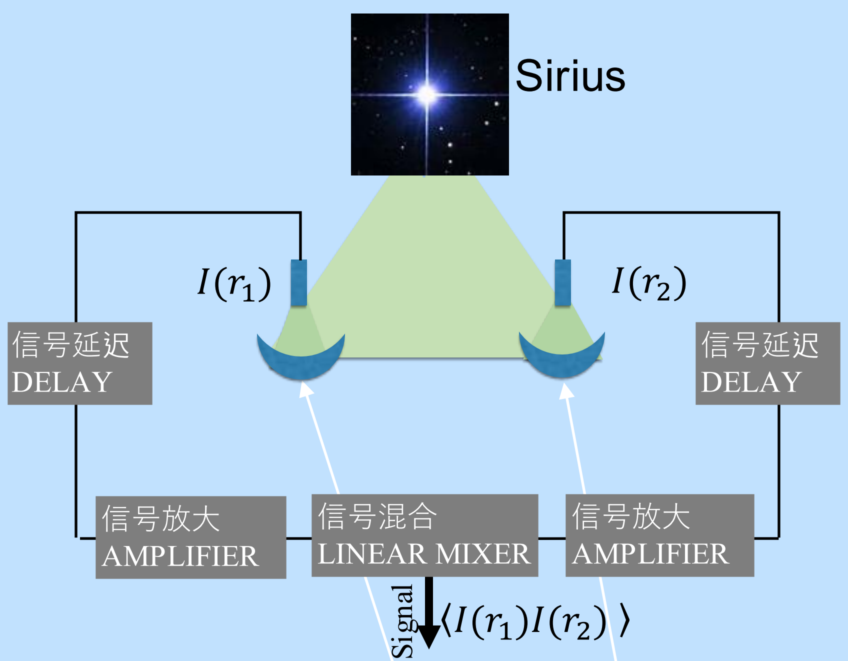


**Average over coincidence measurements**

THE HANBURY BROWN-TWISS INTENSITY INTERFEROMETER AT NARRABRI, NEW SOUTH WALES, AUSTRALIA

图片来源: http://quantumtantra.com/quim.html


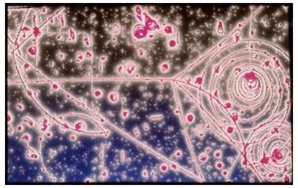

**Sirius angular size**: 0.0063”

Hanbury Brown R 1956 A test of new type of new steller interferometer on SIRIUS *Nature* **178**

$$g^{(2)}(r_1,r_2) = \frac{\langle I(r_1)I(r_2)\rangle}{\langle I(r_1)\rangle\langle I(r_2)\rangle}$$

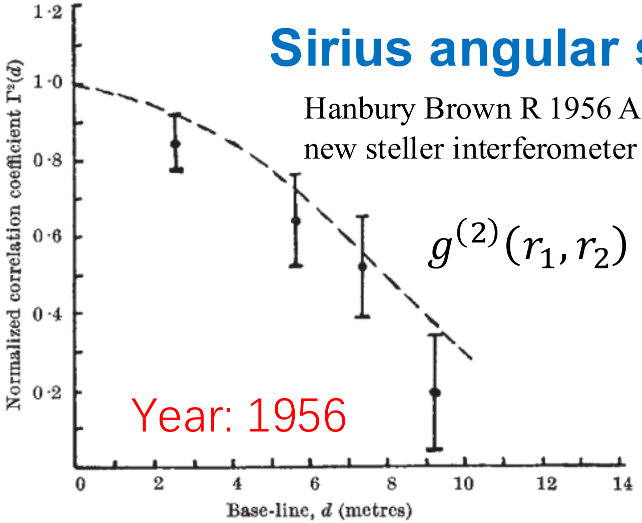


Fig. 2. Comparison between the values of the normalized correlation coefficient Γ²(d) observed from Sirius and the theoretical values for a star of angular diameter 0·0063″. The errors shown are the probable errors of the observations

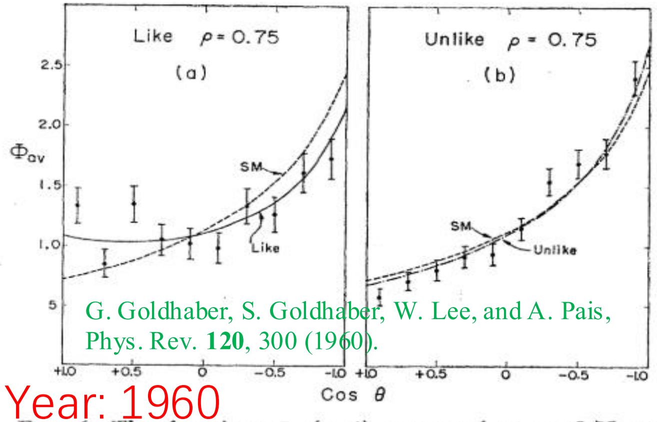


Fig. 6. The functions $\Phi_{av}(\cos\theta)$ computed at $\rho$=0.75 are compared with the experimental distribution of angles between pion pairs. Figures 6(a) and 6(b) give the distributions for like and unlike pions respectively. Also shown in each is the curve for $\Phi_{av}^{SM}(\cos\theta)$, the statistical distribution, without the effect of correlation functions. Here $\Phi_{av}$ represents an average of $\Phi_4$, $\Phi_5$, and $\Phi_6$, weighted according to the individual charge channels. The experimental data comes from reference 1 (see also Table I, footnote a).


Lawrence Radiation Laboratory and Department of Physics, University of California, Berkeley, California

# $\pi^0\pi^0$ correlations | Motivation

## Very few $\pi^0\pi^0$ correlations measurements so far

Table 1: The two-pion emitter dimension $r_2$ and the chaoticity parameter $\lambda_2$ obtained from Bose-Einstein Correlation (BEC) analysis for a variety of hadron reactions. The data marked with a superscribe $^a$ indicats the choice for the reference sample is the $\pi^+\pi^-$ data sample, while $^b$ means the reference samples are either Monte Carlo generated events or a sample constructed by the event mixing technique.

| $BE - System$ | Reaction | Experiment | $E_{cm}$ | $r_2(fm)$ | $\lambda_2$ |
|---|---|---|---|---|---|
| $\pi^\pm\pi^\pm$ | $e^+e^- \to h$ | MARK II [2] | 29 | $0.75 \pm 0.05^a$ | $0.28 \pm 0.04^a$ |
| | | | | $0.97 \pm 0.11^b$ | $0.27 \pm 0.04^b$ |
| $\pi^\pm\pi^\pm$ | $e^+e^- \to h$ | TPC [3] | 29 | $0.65 \pm 0.06^b$ | $0.50 \pm 0.04^b$ |
| $\pi^\pm\pi^\pm$ | $e^+e^- \to h$ | TASSO [4] | 34 | $0.82 \pm 0.07^a$ | $0.35 \pm 0.03^a$ |
| $\pi^\pm\pi^\pm$ | $e^+e^- \to h$ | AMY [5] | 58 | $0.73 \pm 0.21^a$ | $0.47 \pm 0.07^a$ |
| | | | | $0.58 \pm 0.06^b$ | $0.39 \pm 0.05^b$ |
| $\pi^\pm\pi^\pm$ | $e^+e^- \to h$ | ALEPH [6] | 91 | $0.82 \pm 0.04^a$ | $0.48 \pm 0.03^a$ |
| | | | | $0.52 \pm 0.02^b$ | $0.30 \pm 0.01^b$ |
| $\pi^\pm\pi^\pm$ | $e^+e^- \to h$ | DELPHI [7] | 91 | $0.83 \pm 0.03^a$ | $0.31 \pm 0.02^a$ |
| | | | | $0.47 \pm 0.03^b$ | $0.24 \pm 0.02^b$ |
| $\pi^\pm\pi^\pm$ | $e^+e^- \to h$ | L3 [8] | 91 | $0.46 \pm 0.02^b$ | $0.29 \pm 0.03^b$ |
| $\pi^\pm\pi^\pm$ | $e^+e^- \to h$ | OPAL [1] | 91 | $0.96 \pm 0.02^a$ | $0.67 \pm 0.03^a$ |
| | | | | $0.79 \pm 0.02^b$ | $0.58 \pm 0.01^b$ |
| $\pi^\pm\pi^\pm$ | $\gamma\gamma \to h$ | [2] | 5 | $1.05 \pm 0.08$ | $1.20 \pm 0.13$ |
| $\pi^\pm\pi^\pm$ | $\gamma\gamma \to 6\pi^\pm$ | [11] | 1.6-7.5 | $0.54 \pm 0.22$ | $0.59 \pm 0.20$ |
| $\pi^\pm\pi^\pm$ | $\nu(\bar{\nu})N \to h$ | [12] | 8-64 | $0.64 \pm 0.16$ | $0.46 \pm 0.16$ |
| $\pi^\pm\pi^\pm$ | $\mu p \to h$ | [13] | 23 | $0.65 \pm 0.03$ | $0.80 \pm 0.07$ |
| $\pi^\pm\pi^\pm$ | $\pi^+ p \to h$ | [14] | 21.7 | $0.83 \pm 0.06$ | $0.33 \pm 0.02$ |
| $\pi^\pm\pi^\pm$ | $pp \to h$ | [15] | 26 | $1.02 \pm 0.20$ | $0.32 \pm 0.08$ |
| $\pi^\pm\pi^\pm$ | $pp \to h$ | [16] | 27.4 | $1.20 \pm 0.03$ | $0.44 \pm 0.01$ |
| $\pi^\pm\pi^\pm$ | $pp \to h$ | [17] | 63 | $0.82 \pm 0.05$ | $0.40 \pm 0.03$ |
| $\pi^\pm\pi^\pm$ | $\bar{p}p \to h$ | [18] | 1.88 | $1.04 \pm 0.01$ | $1.96 \pm 0.03$ |
| $\pi^\pm\pi^\pm$ | $\bar{p}p \to h$ | [19] | 200-900 | $0.73 \pm 0.03$ | $0.25 \pm 0.02$ |
| $\pi^\pm\pi^\pm$ | $ep \to eh$ | [20] | $2.45 < Q_\gamma < 10$ | $0.68 \pm 0.06$ | $0.52 \pm 0.20$ |
| $\pi^\pm\pi^\pm$ | $ep \to eh$ | [21] | $10.5 < Q_\gamma$ | $0.67 \pm 0.04$ | $0.43 \pm 0.09$ |
| $\pi^0\pi^0$ | $e^+e^- \to h$ | L3 [8, 9] | 91 | $0.31 \pm 0.10^b$ | $0.16 \pm 0.09^b$ |
| $\pi^0\pi^0$ | $e^+e^- \to h$ | OPAL [10] | 91 | $0.59 \pm 0.11^b$ | $0.55 \pm 0.15^b$ |
| $k^\pm k^\pm$ | $ep \to eh$ | [22] | $E_e : 27.5; E_p : 820$ | $0.37 \pm 0.07^{+0.09}_{-0.08}$ | $0.57 \pm 0.09^{+0.15}_{-0.08}$ |
| $k^0_S k^0_S$ | $ep \to eh$ | [22] | $E_e : 27.5; E_p : 820$ | $0.70 \pm 0.19^{+0.28+0.38}_{-0.08-0.52}$ | $0.63 \pm 0.09^{+0.07+0.09}_{-0.08-0.02}$ |

$\pi^0\pi^0$ correlations

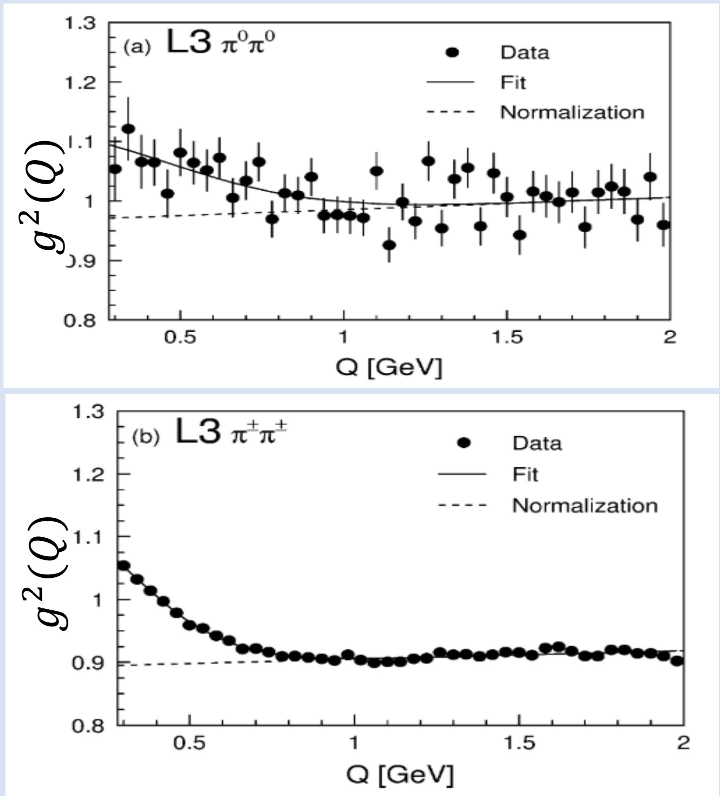


Fig. 4. Distribution of $g^2(Q)$ for (a) π0π0 and (b) π±π±, and results of the fits. The points indicate the data, the full line corresponds to the fit result and the dashed line is the normalization factor N(1 +αQ).

source: Achard P, et al 2002 Bose–Einstein correlations of neutral and charged pions in hadronic Z decays *Phys. Lett. B* **524** 55–64

# Intensity interference of bosons:

## Bose-Einstein correlations (BEC)

space-time properties ⇕ enhancement

Size ?

~ 0.000000000000001 m

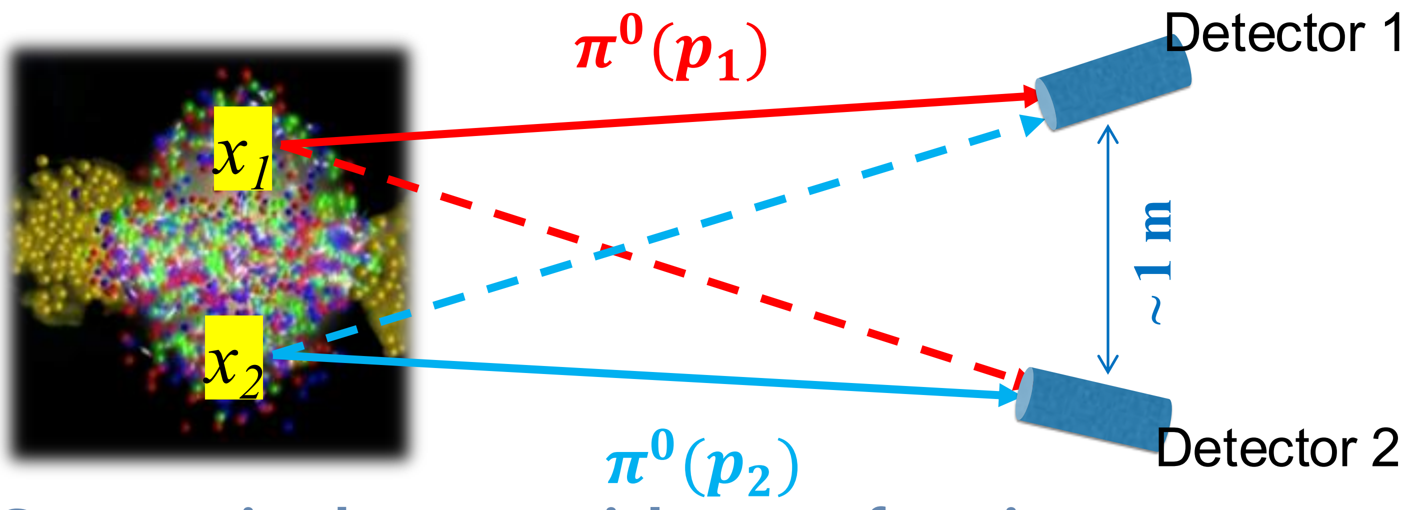


**Symmetrized two-particle wave function**

$$\psi^s = \frac{1}{\sqrt{2}}\left[e^{-i(p_1(d_1-x_1)+p_2(d_2-x_2))} + e^{-i(p_1(d_1-x_2)+p_2(d_2-x_1))}\right]$$

*(assume plane wave function of propagation)*

This **symmetrization** results in an **enhanced probability** $(P_{12}(p_1,p_2) = \langle\psi^{s*}\psi^{S}\rangle)$ of emission if the two bosons have similar momenta.

# Correlation function

measured in terms of a **correlation function:**

$$C_2(p_1, p_2) \equiv \frac{P_{12}(p_1, p_2)}{P_1(p_1)P_2(p_2)}$$

completely chaotic:

$$C_2(p_1, p_2) = 1 + |\hat{\rho}(Q)|^2$$

completely coherent:

$$C_2(p_1, p_2) = 1$$

$$C_2(Q) = N(1 + \lambda_2 e^{r_0^2 Q^2})$$

N: normalized factor
**$r_0$** : emitter radius
**$\lambda_2$** : chaoticity parameter ($0 \leqq \lambda_2 \leqq 1$)
0: completely coherent case
1: totally chaotic limit

$Q^2 = -(p_1 - p_2)^2$
$p_{1,2}$: four momentum of the two identical particles.

Assume the particle emitting source has a Gaussian profile of density distribution

$$\rho(x) = \rho(0)e^{-x^2/2r_0^2}$$

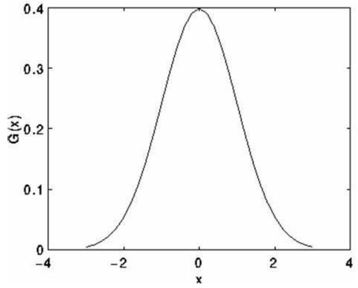


$\hat{\rho}(Q)$: Normalized Fourier transform of source density ρ(x):

$$\hat{\rho}(Q) = \int dx \rho(x) e^{i(p_1 - p_2)x} \qquad |\hat{\rho}(Q)|^2 = e^{r_0^2 Q^2}$$

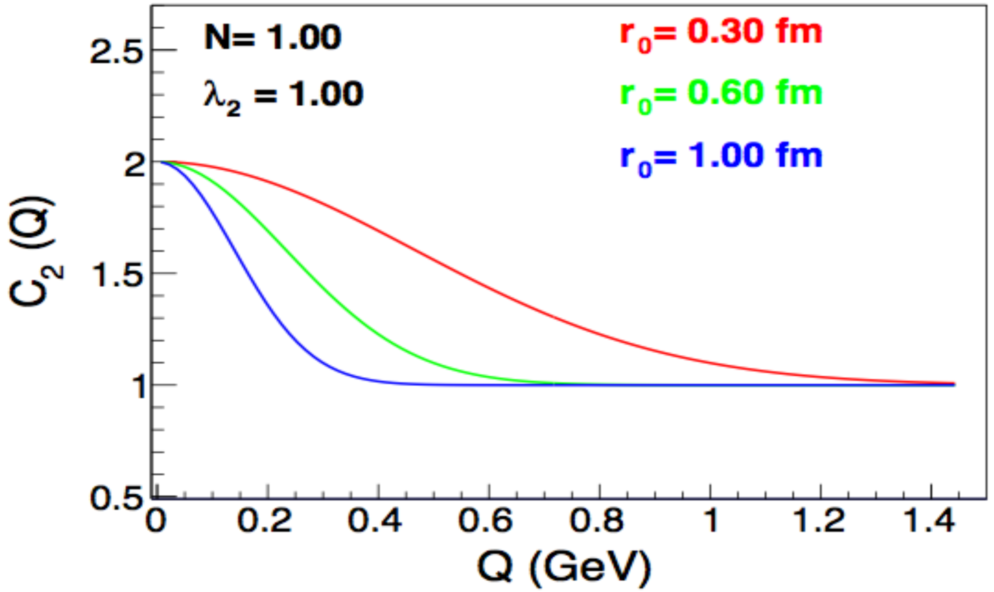

# $\pi^0\pi^0$ correlations | Event selection

$$\gamma p \rightarrow \pi^0\pi^0 p \rightarrow \gamma\gamma\gamma\gamma p$$

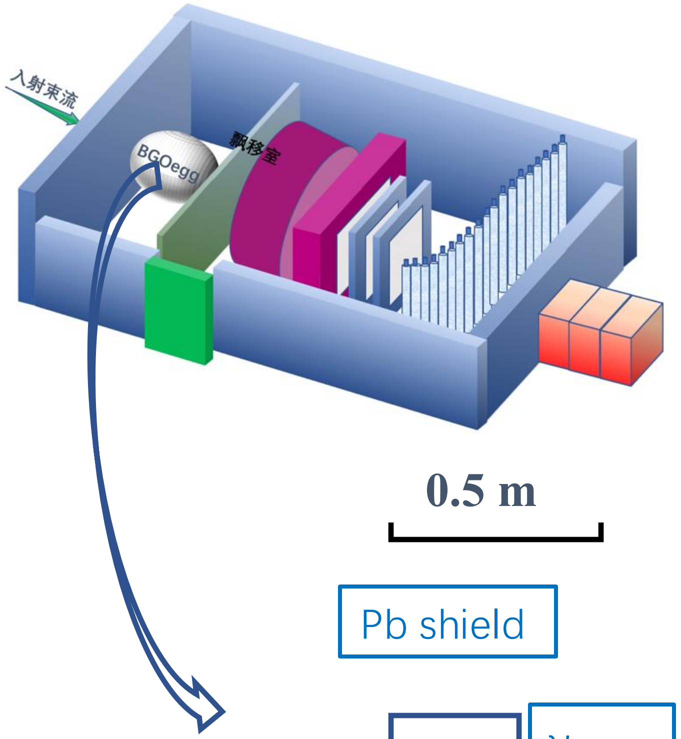


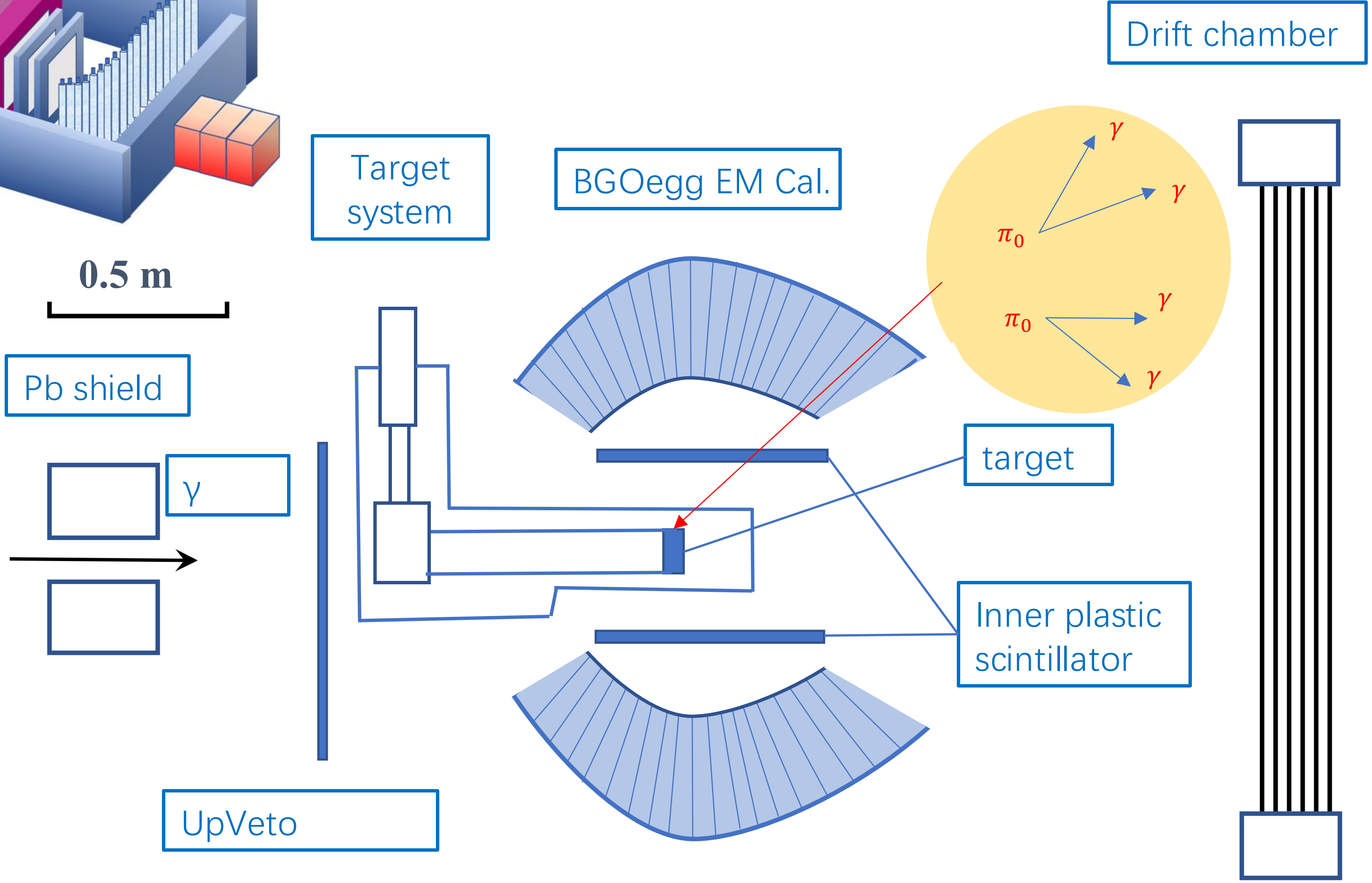


**BGOegg**

- 1320 BGOcrystals
- Polar coverage: 24°-144°
- EM cluster energy threshold: 30 MeV
- 2 hits $\Delta t < 2$ ns

**Planner drift chamber**

Polar coverage: $\theta < 21°$

**Tagged beam photons**

reaches $3.320 \times 10^{12}$ with the correction for dead times.

**4 neutral clusters**
**1 charged particle hit**

# $\pi^0\pi^0$ correlations | Event selection

(1) $4\gamma s$ detected by the BGOegg as neutral particles

**Energy threshold**: 30 MeV

**Timing difference** of any two gammas: <2 ns

(2) A proton was detected as a charged cluster in **BGO** or a straight track in the planar **drift chamber**.

(3) A kinematic fit with the constraints of four-momentum conservation and $\pi^0$ mass was also used to inspect the selected events.

$\chi^2$ **probabilities** cut: >2%

(4) BGO layer cut

The **most-forward** or **most-backward layer** of the calorimeter was not used in gamma detection to avoid a problem of large energy leak.

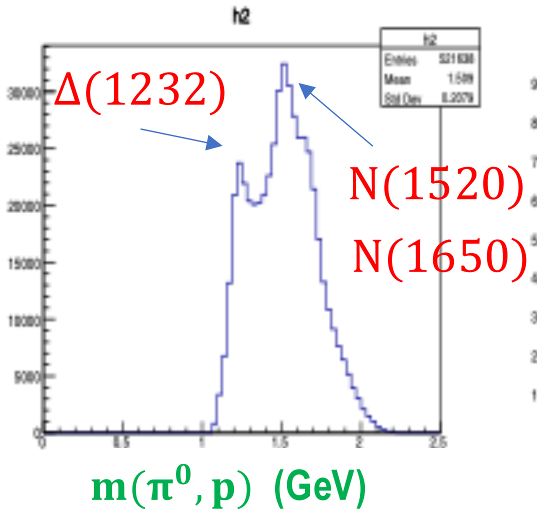


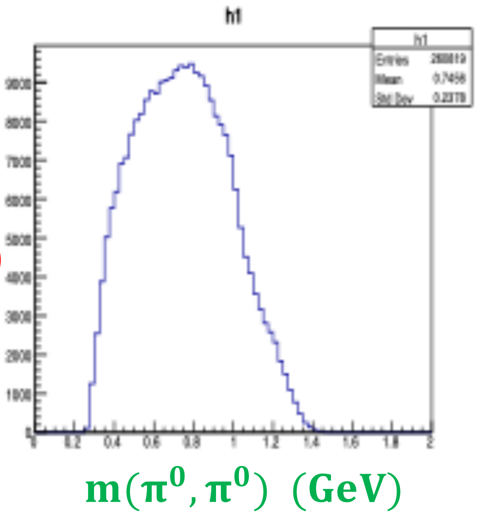


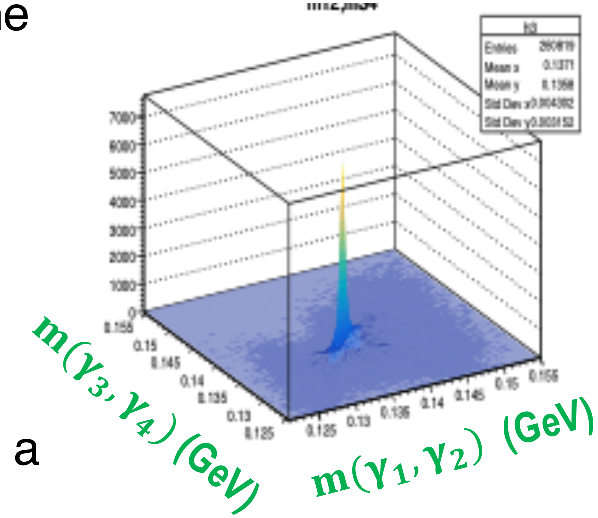

# $\pi^0\pi^0$ correlations | Event selection

- **6 constraints KF**

\- **2 $\pi^0$** masses (2C)

\- **Four momentum conservation (4c)**

- $P(\chi^2) > 1\%$

## Kinematic fitting

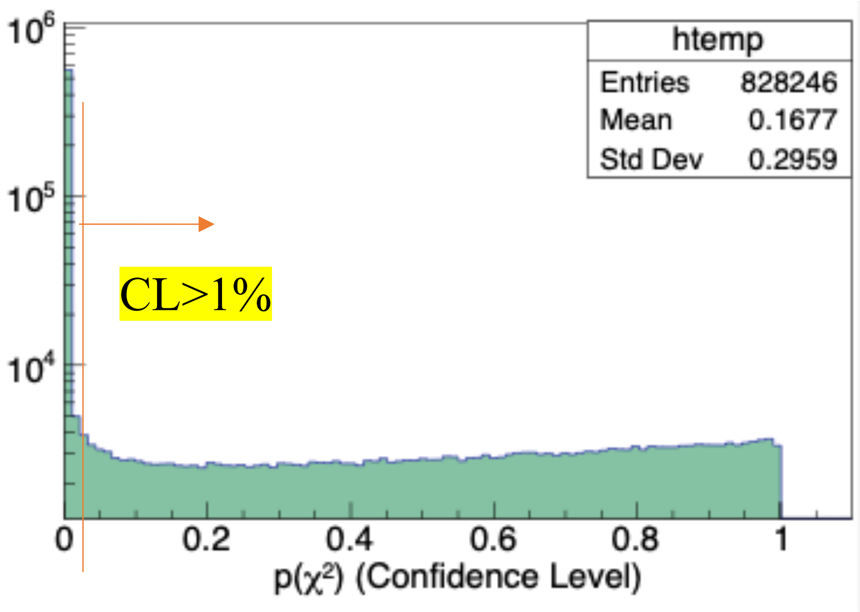


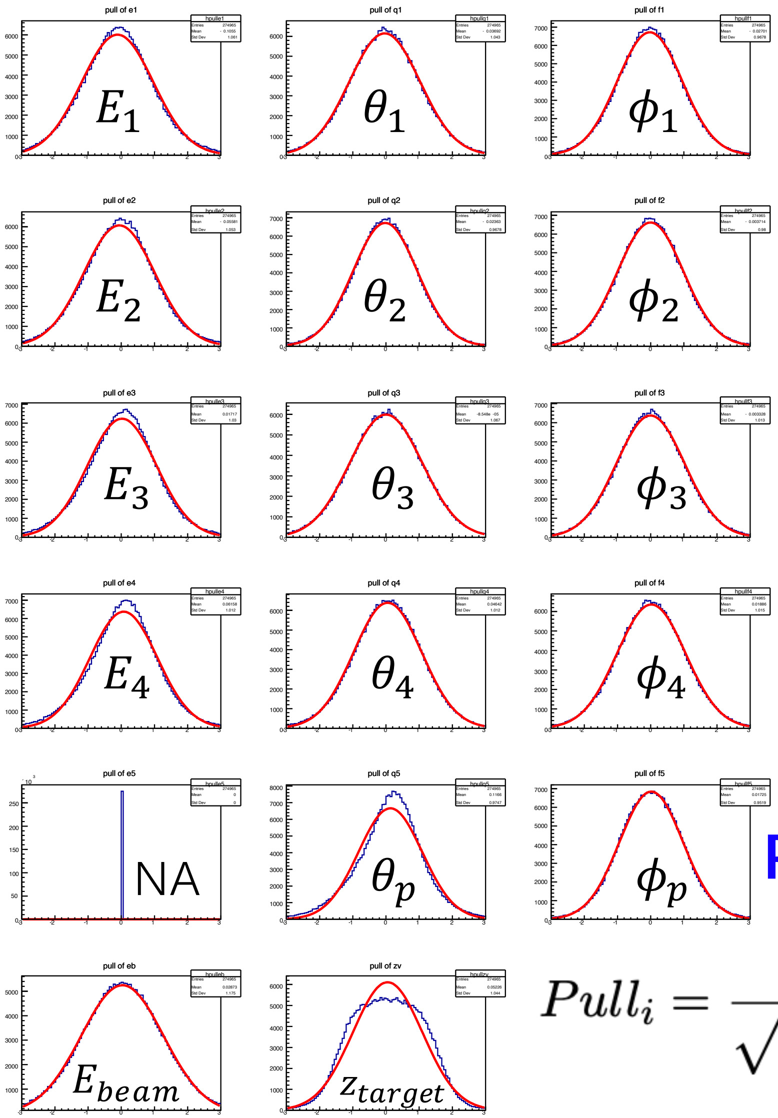


Gaus(0,1)

BGOegg

## Pull distribution

$$Pull_i = \frac{(\eta_i - y_i)}{\sqrt{(\sigma^2(\eta_i) - \sigma^2(y_i))}}$$

# $\pi^0\pi^0$ correlations | Correlation function

$$C_2(Q) = \frac{P_{BE}(Q)}{P_{noBE}(Q)} = \frac{r_{BE}(Q)}{r_{noBE}(Q)}$$

Signal sample

reference sample (event mixing)

$$Q^2 = -(p_1 - p_2)^2 = (p_1 + p_2)^2 - 4m^2$$

**Challenges of event mixing at low energies with low multiplicities.**

| **low** energies<br>**low** multiplicities | **high** energies<br>**high** multiplicities |
|---|---|
| **strongly disturbed** by non-BEC factors of exclusive reactions with a low multiplicity such as **global conservation laws** and decays of **resonances** 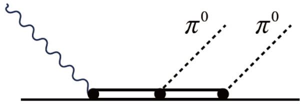  | **weakly disturbed** by non-BEC factors such as **global conservation laws** |
| Complicated kinematical constraints | Simple kinematical constraints |

## (1) Appropriate mixing constraints for $\pi^0\pi^0 p$ system

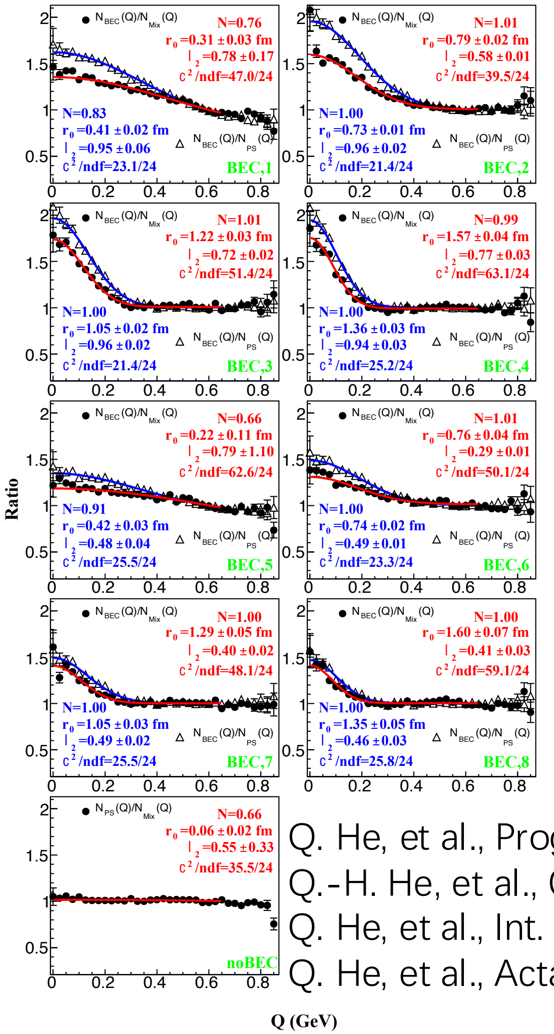


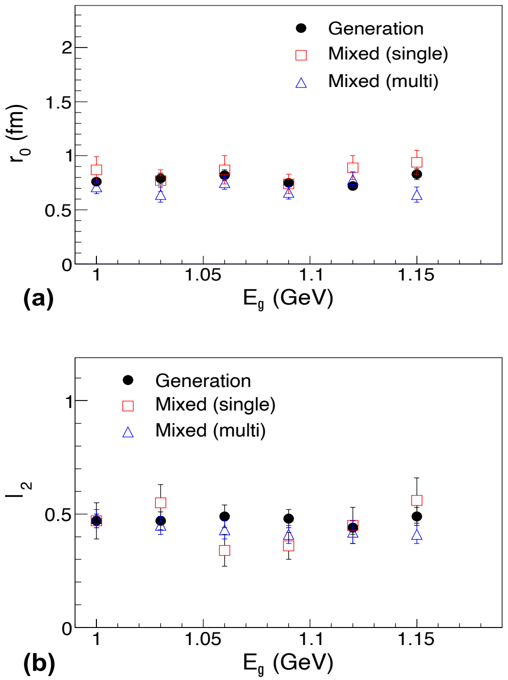


Q. He, et al., Prog. Theor. Exp. Phys. **2017**, (2017)
Q.-H. He, et al., Chinese Phys. C **40**, 114002 (2016)
Q. He, et al., Int. J. Mod. Phys. E. 28, 1950024 (2019)
Q. He, et al., Acta Phys. Pol. B. 51, 463–471 (2020)

## (2) $\gamma p \rightarrow \pi^0 N^* \rightarrow \pi^0\pi^0 p$ influence on c.f.

$$CF_{D.R.}(Q) = \left(\frac{\rho^{exp}_{sig}(Q)}{\rho^{exp}_{mix}(Q)}\right) \Big/ \left(\frac{\rho^{MC}_{sig}(Q)}{\rho^{MC}_{mix}(Q)}\right)$$

# $\pi^0\pi^0$ correlations | Correlation function

$$CF_{D.R.}(Q) = \left(\frac{\rho^{exp}_{sig}(Q)}{\rho^{exp}_{mix}(Q)}\right) \Big/ \left(\frac{\rho^{MC}_{sig}(Q)}{\rho^{MC}_{mix}(Q)}\right)$$

## Case 1: Focus on Δ(1232)

$$|m(p, \pi^0_{low}) - 1232| < 50\ MeV$$

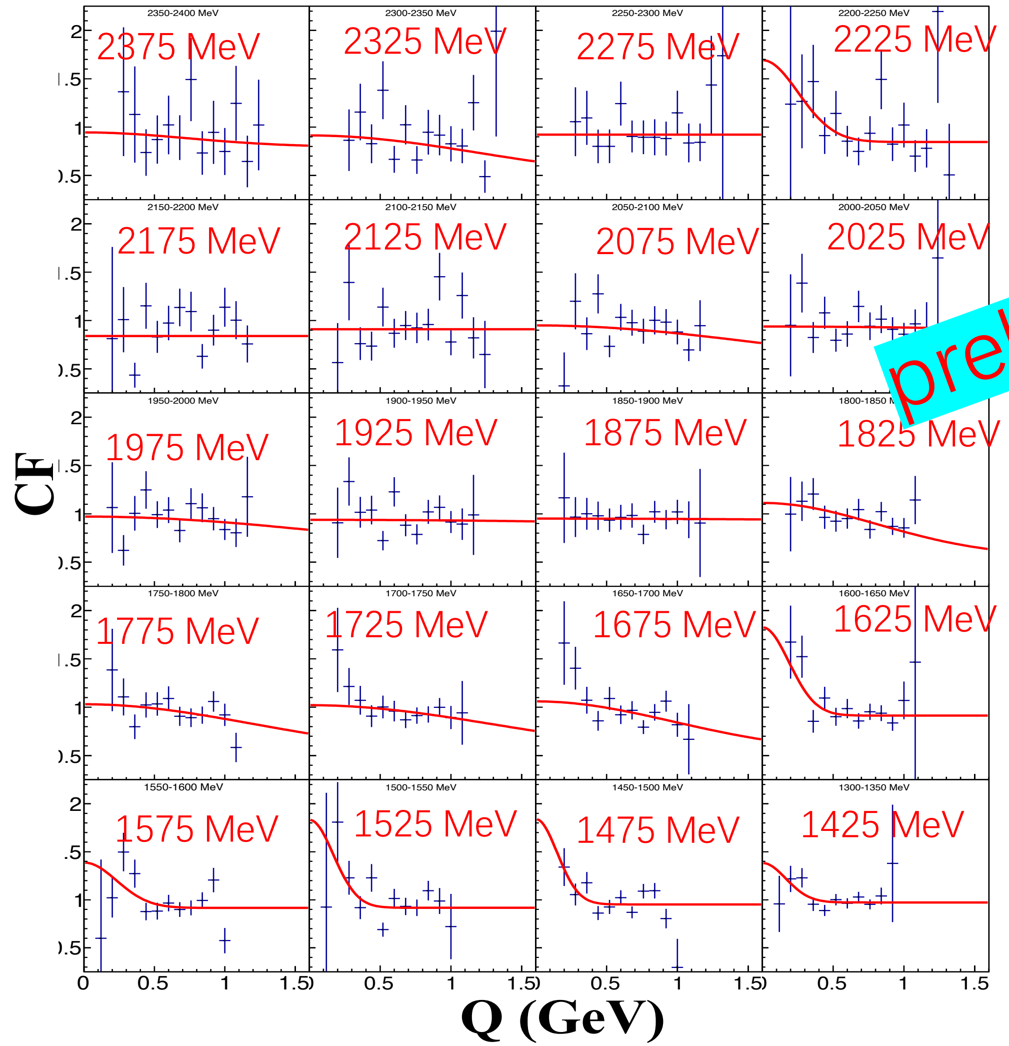


## Case 2: Suppressing $\gamma p \rightarrow \pi^0 N^* \rightarrow \pi^0\pi^0 p$ process

$N^*$: Δ(1232), N(1535), N(1650)

**BGOegg 2014B dataset**

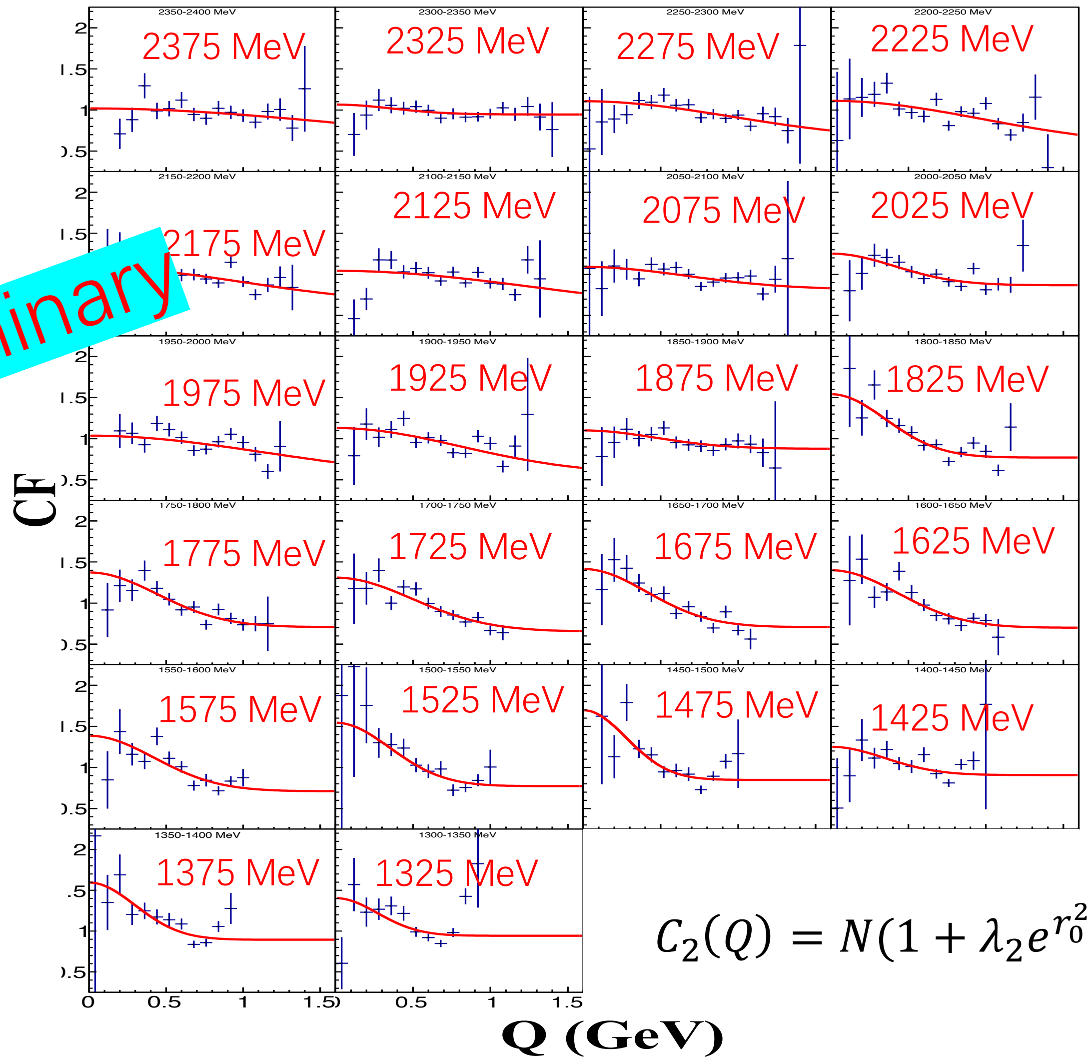


$$C_2(Q) = N(1 + \lambda_2 e^{r_0^2 Q^2})$$

# $\pi^0\pi^0$ correlations | Correlation function

**Case 2: Suppressing $\gamma p \to \pi^0 N^* \to \pi^0\pi^0 p$ process**

BGOegg 2014B dataset

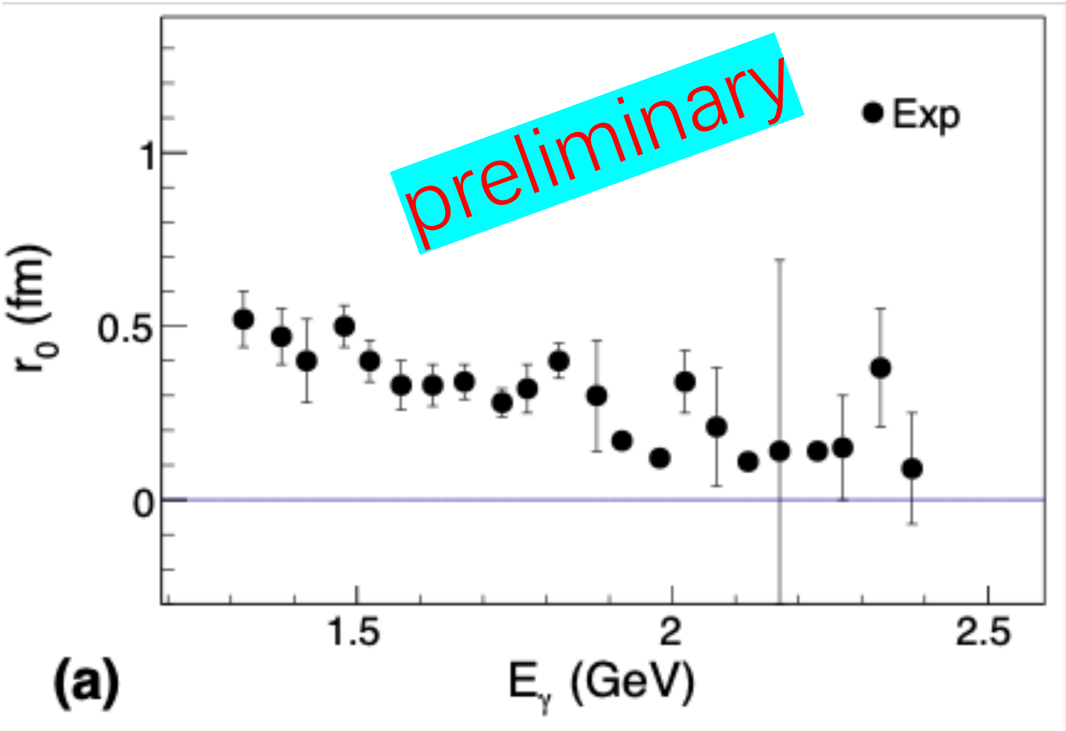


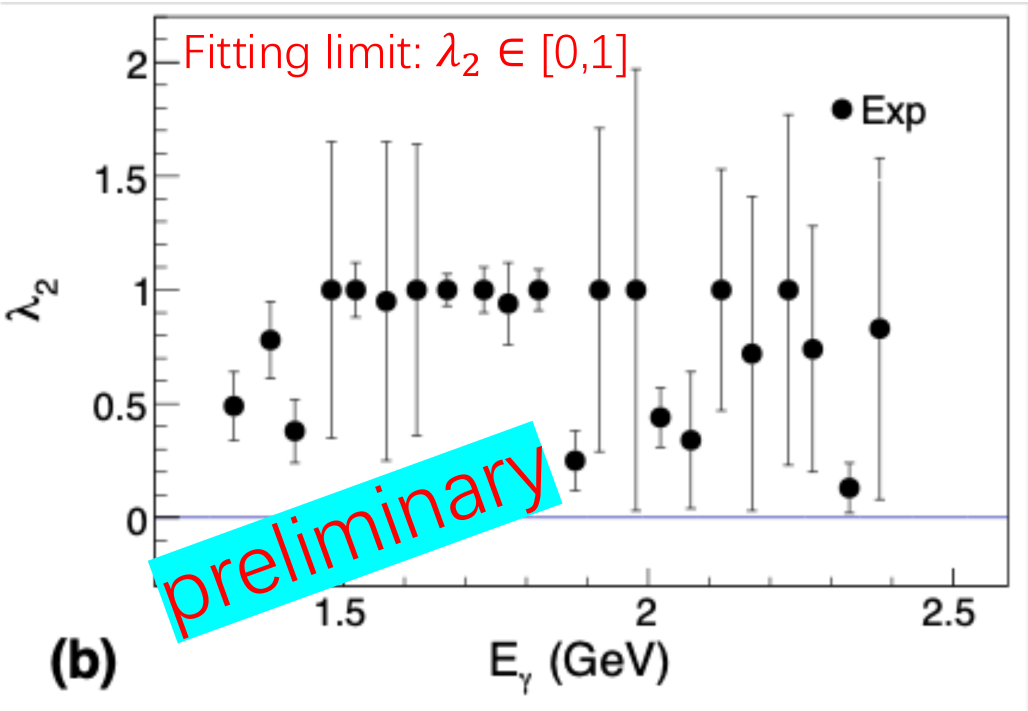


Fit: $C_2(Q) = N(1 + \lambda_2 e^{r_0^2 Q^2})$

# Discussion

## $\pi^0\pi^0$ strong final state interaction through $f_0(500)$ and $f_0(980)$

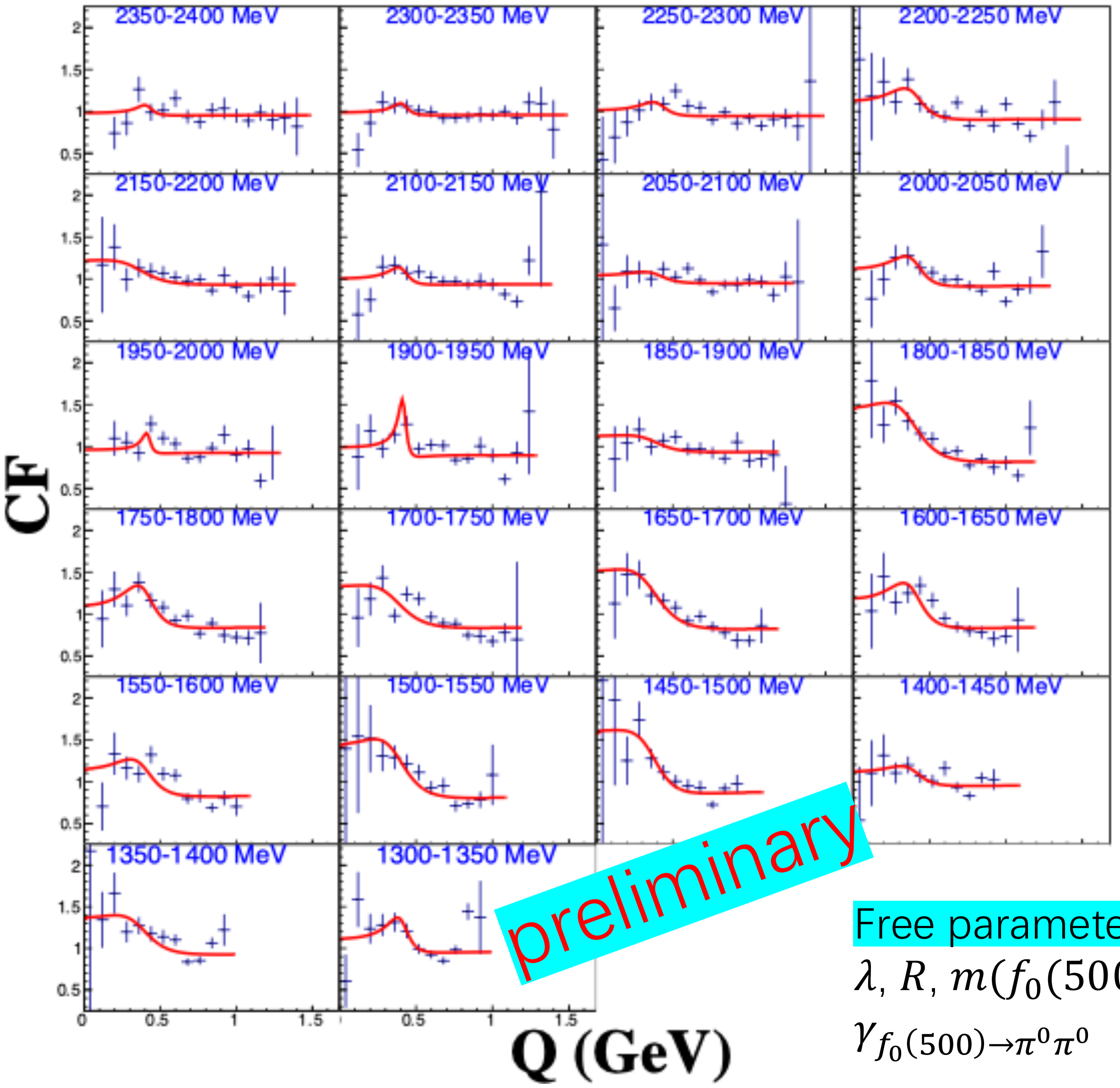


$$C_{Lednicky}(k^*) = 1 + \lambda e^{-4k^{*2}R^2} + \lambda\alpha\left[\left|\frac{f(k^*)}{R}\right|^2 + \frac{4\Re f(k^*)}{\sqrt{\pi}R}F_1(2k^*R) - \frac{2\Im f(k^*)}{R}F_2(2k^*R) + \Delta C\right]$$

$$F_1(z) = \int_0^z dx\,\frac{e^{x^2-z^2}}{z} \qquad F_2(z) = \frac{1-e^{-z^2}}{z}$$

$$f(k^*) = \frac{f_0(k^*) + f_1(k^*)}{2}$$

$$f_I(k^*) = \frac{\gamma_I}{m_I^2 - s - i(\gamma_I k^* + \gamma_I' k_I')}$$

$\Delta C = 0$ for the moment

* ALICE, PLB. 833 (2022) 137335.
* R. Molina, Z.W. Liu, L.S. Geng, E. Oset, EPJC. 84 (2024) 1–8.
* R. Molina, C.W. Xiao, W.H. Liang, E. Oset, ArXiv: 2310.12593

Free parameters:
$\lambda$, $R$, $m(f_0(500))$, $\gamma_{f_0(500)\to\pi^0\pi^0}$

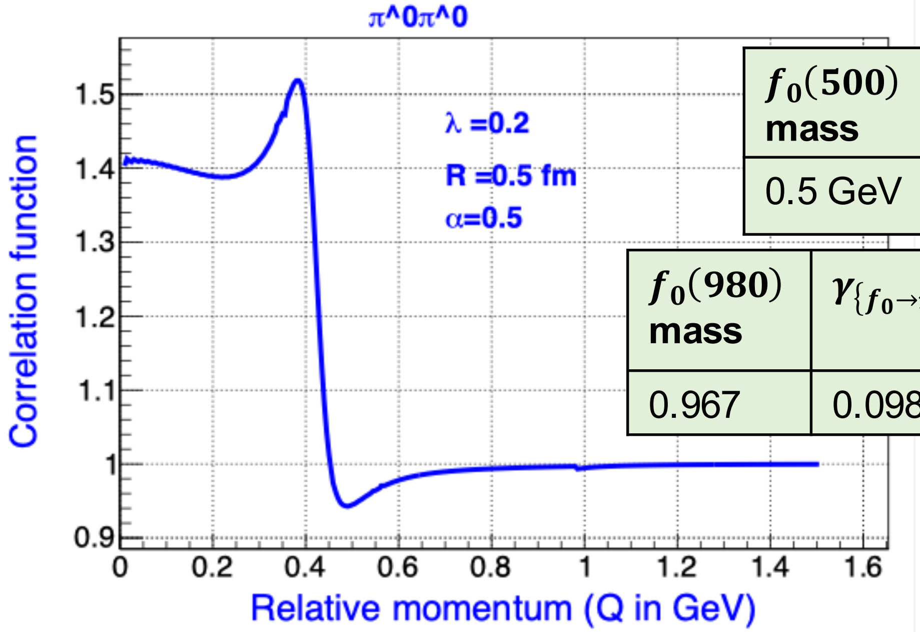


| $f_0(500)$ mass | $\gamma_{\{f_0\to\pi^0\pi^0\}}$ |
|---|---|
| 0.5 GeV | 0.18 GeV |

| $f_0(980)$ mass | $\gamma_{\{f_0\to\pi^0\pi^0\}}$ | $\gamma_{\{f_0\to K\overline{K}\}}$ |
|---|---|---|
| 0.967 | 0.098 | 0.34 |

## Discussion

### $\pi^0\pi^0$ strong final state interaction through $f_0(500)$ and $f_0(980)$

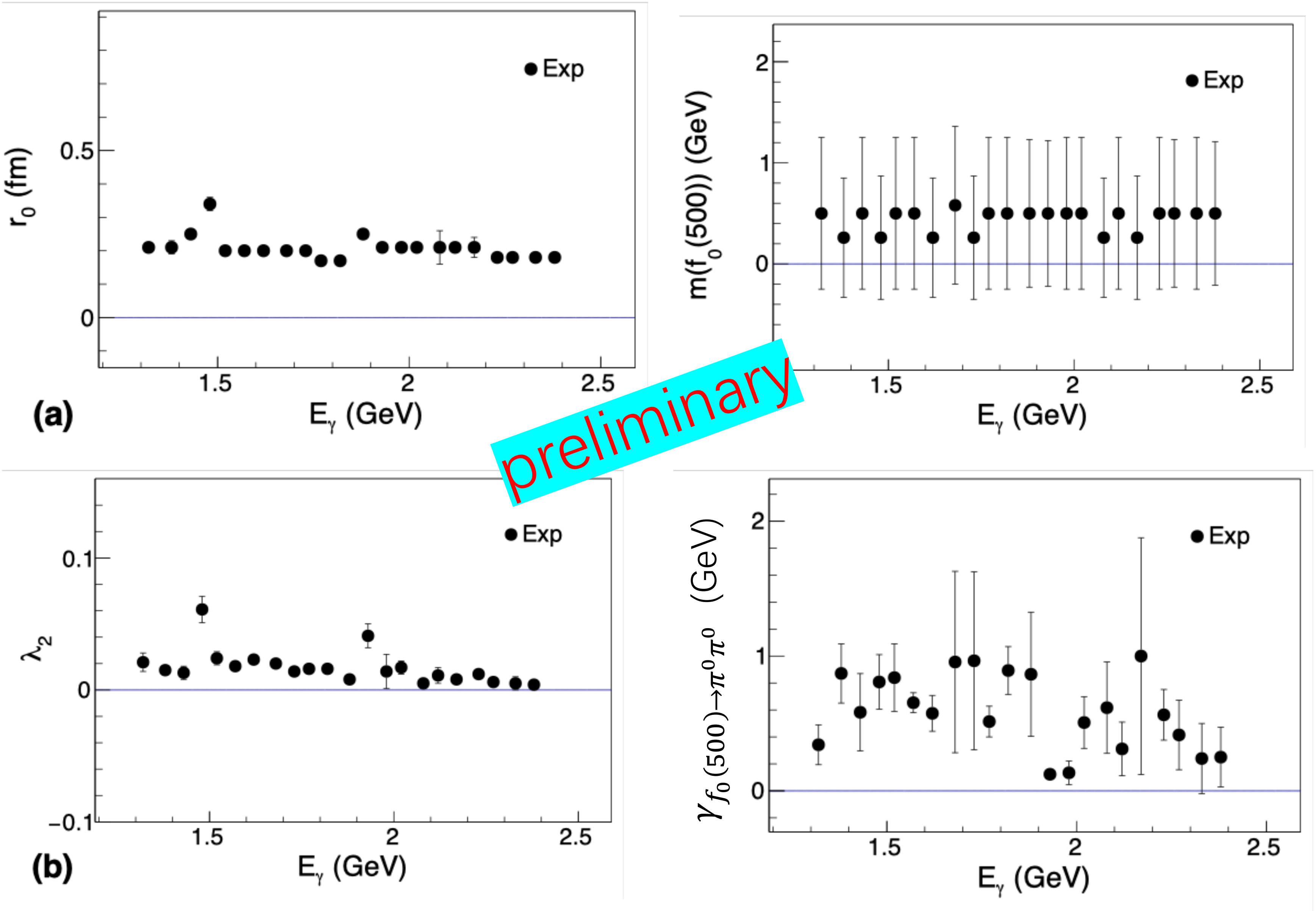


Free parameters:

$\lambda \in [0,1]$

$R \in$: [0,2] fm

$m(f_0(500)) \in$: [0,1] GeV

$\gamma_{f_0(500)\to\pi^0\pi^0} \in$: [0.1, 1.0] GeV

# Discussion

## (2) $\gamma p \to \pi^0 N^* \to \pi^0\pi^0 p$ influence on c.f.

- S wave meson emission due to an energetic quark

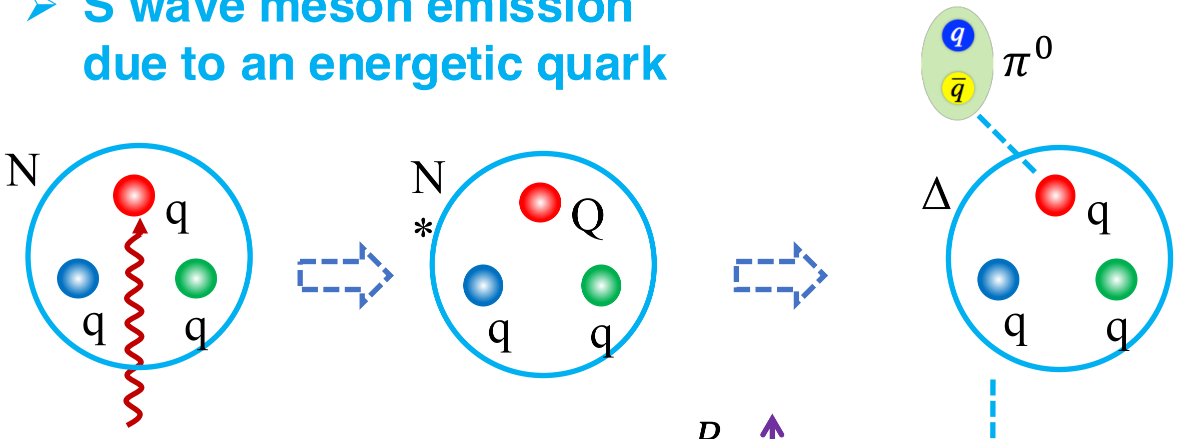


- Δ→π$^0$N decay originated by an energetic quark Q

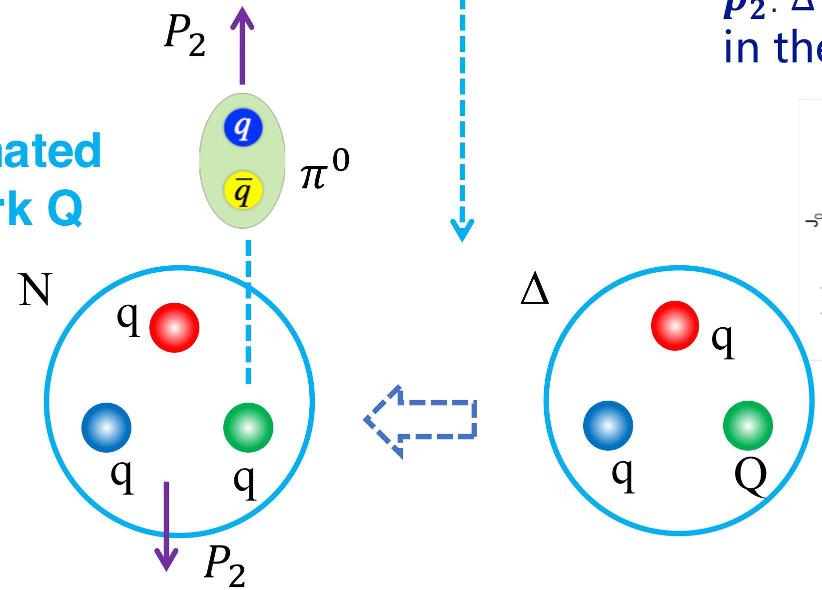


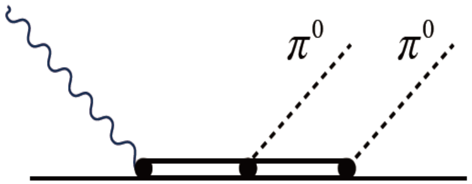


H. Shimizu, ELPH Annual Report, 2017
Q. He, J. Phys. Conf. Ser. 1643, 012010 (2020).

$$C_{BEC}(q,p_2) = 1 + \lambda \exp\left(-\frac{\alpha^2 q^2}{2}\right) \exp\left(-\frac{\alpha^2 q_z^2}{2}\right) J_0(\beta q_r)$$
$$= 1 + \lambda \exp(-\alpha^2 q_z^2) \exp\left(-\frac{\alpha^2 q_r^2}{2}\right) J_0(\beta q_r)$$

$q$: relative momentum of two pions in the frame of Δ at rest

$\vec{q} = (q_r, 0, q_z)$ in cylindrical coordinates $\quad \beta = \frac{1}{2p_2}$

$J_0(\beta q_r)$: 0th-order Bessel function

$p_2$: Δ decayed pion 3-d momentum in the frame of Δ at rest

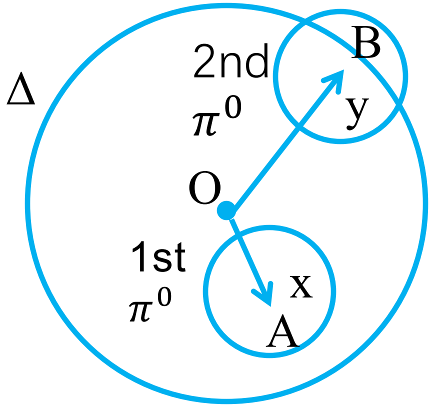


Space-time coordinates of Δ at rest

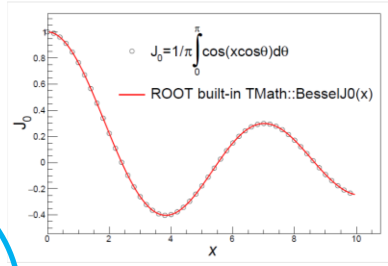


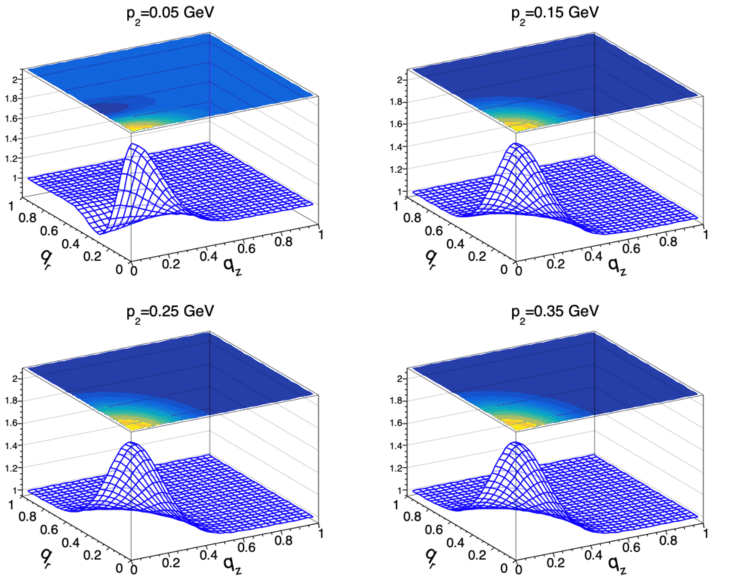


More statistics is required

# Summary

- The preliminary results in case (1) (focusing on $\Delta$) shows the correlation strength is very weak (almost 0) in the beam energy region of 1.3-2.4 GeV.
- The preliminary results in case (2) (suppressing sequential decay) indicate the pi-pi correlations strength decreases as beam energy increases. Since $\pi^0 N^*$ or $\pi^0\Delta$ sequential processes are suppressed in case2, the possible reason for this phenomenon is that the contribution of the processes ($f_0(500)$ and $f_0(980)$) directly decaying to two pions becomes smaller when the beam energy increases from 1.3 to 2.4 GeV.
- Including strong final state interaction of $\pi^0\pi^0$ through the $f_0(500)$ and $f_0(980)$ resonance may provide more interesting information

# Thank you!